A dual role for K63-linked ubiquitin chains in multivesicular body biogenesis and cargo sorting

Zoi Erpapazoglou[a,*], Manel Dhaoui[a,†,‡], Marina Pantazopoulou[a,†,§], Francesca Giordano[b,‖], Muriel Mari[c], Sébastien Léon[a], Graça Raposo[b], Fulvio Reggiori[c], and Rosine Haguenauer-Tsapis[a]

[a]Institut Jacques Monod, Centre National de la Recherche Scientifique, Unité Mixte de Recherche 7592, Université Paris-Diderot, Sorbonne Paris Cité, F-75205 Paris, France; [b]Institut Curie, Centre de Recherche, F-75248 Paris, France; [c]University Medical Centre Utrecht, 3584C Utrecht, Netherlands

ABSTRACT **In yeast, the sorting of transmembrane proteins into the multivesicular body (MVB) internal vesicles requires their ubiquitylation by the ubiquitin ligase Rsp5. This allows their recognition by the ubiquitin-binding domains (UBDs) of several endosomal sorting complex required for transport (ESCRT) subunits. K63-linked ubiquitin (K63Ub) chains decorate several MVB cargoes, and accordingly we show that they localize prominently to the class E compartment, which accumulates ubiquitylated cargoes in cells lacking ESCRT components. Conversely, yeast cells unable to generate K63Ub chains displayed MVB sorting defects. These properties are conserved among eukaryotes, as the mammalian melanosomal MVB cargo MART-1 is modified by K63Ub chains and partly missorted when the genesis of these chains is inhibited. We show that all yeast UBD-containing ESCRT proteins undergo ubiquitylation and deubiquitylation, some being modified through the opposing activities of Rsp5 and the ubiquitin isopeptidase Ubp2, which are known to assemble and disassemble preferentially K63Ub chains, respectively. A failure to generate K63Ub chains in yeast leads to an MVB ultrastructure alteration. Our work thus unravels a double function of K63Ub chains in cargo sorting and MVB biogenesis.**

Monitoring Editor
Sandra Lemmon
University of Miami

Received: Oct 31, 2011
Revised: Mar 23, 2012
Accepted: Mar 30, 2012

INTRODUCTION

Ubiquitylation, the process by which ubiquitin (Ub) is conjugated to target substrates, plays a major role in intracellular protein degradation by both the proteasome and the lysosome/vacuole. Proteins can be modified by the addition of a single Ub molecule to one (monoubiquitylation) or several (multi-monoubiquitylation) lysine residues. Alternatively, Ub molecules can be ligated to each other to form chains in which each monomer is linked to a lysine residue of the previous Ub moiety (polyubiquitylation). Ub harbors seven lysine residues (K6, K11, K27, K29, K33, K48, and K63), all of which can be used to generate a Ub chain (Weissman, 2001). Studies have indicated that poly-Ub chains linked via the Lys-48 (K48) residue of Ub are recognized by several ubiquitin-binding domain (UBD)–containing proteasomal subunits, mediating the targeting of substrates to the proteasome (Glickman and Ciechanover, 2002). Other types of Ub chains have also recently been implicated in the degradation of proteasomal substrates, but no such role has been reported for K63-linked ubiquitin (K63Ub) chains (Xu *et al.*, 2009), which are involved in many key cellular functions, including translation, DNA repair, kinase activation, and trafficking (reviewed in Weissman, 2001).

In yeast, a number of endocytic cargo proteins are linked to short K63Ub chains at the plasma membrane (reviewed in Belgareh-Touze *et al.*, 2008). This modification, mediated by Rsp5, the only member of the Nedd4 protein family of E3 Ub ligases in yeast (Galan *et al.*, 1996; Dupre *et al.*, 2004), is required for efficient internalization (Galan and Haguenauer-Tsapis, 1997; Paiva *et al.*, 2009). Various endocytic cargoes are also modified by K63Ub chains in mammalian cells (Belgareh-Touze *et al.*, 2008), resulting in their

This article was published online ahead of print in MBoC in Press (http://www.molbiolcell.org/cgi/doi/10.1091/mbc.E11-10-0891) on April 4, 2012.

†These authors contributed equally to this work.

Present addresses: *Institut de Biologie Physico-Chimique, 75005 Paris, France; ‡Laboratoire de Biologie Moléculaire de la Cellule, Ecole Normale Supérieure de Lyon, 69364 Lyon, France; §The Wenner-Gren Institute for Experimental Biology, 10691 Stockholm, Sweden; ‖Department of Cell Biology, Yale University School of Medicine, New Haven, CT 06510.

Address correspondence to: Rosine Haguenauer-Tsapis (haguenauer@ijm.univ-paris-diderot.fr).

Abbreviations used: DUB, deubiquitylating enzyme; ESCRT, endosomal sorting complex required for transport; K63Ub chains, K63-linked ubiquitin chains; ILVs, intraluminal vesicles of multivesicular bodies; MVBs, multivesicular bodies; Ub, ubiquitin; UBD, ubiquitin-binding domain.

rapid internalization (Duncan *et al.*, 2006). Ubiquitylation also constitutes a signal for the targeting of both biosynthetic transmembrane proteins and endocytic cargoes into the intraluminal vesicles (ILVs) of multivesicular bodies (MVBs; Katzmann *et al.*, 2002). Rsp5 is the main E3 involved in the ubiquitylation of MVB cargoes (Dunn *et al.*, 2004; Katzmann *et al.*, 2004; Morvan *et al.*, 2004). A few MVB cargoes were shown to be modified by K63Ub chains (Stawiecka-Mirota *et al.*, 2007; Lauwers *et al.*, 2009), and cells unable to assemble this type of Ub chain display an impairment of MVB sorting of some endocytic and MVB cargoes (reviewed in Lauwers *et al.*, 2010). The modification of both endocytic and MVB substrates by K63Ub chains is consistent with the predominant mode of K63Ub chain generation by Rsp5 due to the structural properties of its catalytic domain (Kee *et al.*, 2005, 2006). Some human members of the Nedd4 protein family have a similar structure and also assemble K63Ub chains (Kim and Huibregtse, 2009; Kim *et al.*, 2011; Maspero *et al.*, 2011).

Ub chains on endocytic and MVB cargoes are recognized by receptors carrying UBDs (Katzmann *et al.*, 2002; Raiborg and Stenmark, 2009). For example, MVB cargoes are captured by the endosomal sorting complex required for transport (ESCRT) machinery, a conserved system of interacting complexes crucial for MVB biogenesis and sorting (Katzmann *et al.*, 2002). Ub linked to the cargoes is initially recognized by UBDs present in the two proteins forming the ESCRT-0 complex, Vps27 and Hse1, known as Hrs and STAM, respectively, in mammals. The ubiquitylated cargo is then concentrated by the action of the UBD-containing proteins of the ESCRT-I and -II complexes and guided into membrane invaginations that form from the limiting membrane of endosomes. After ESCRT-III–mediated membrane abscission, these invaginations become ILVs (Katzmann *et al.*, 2002; Raiborg and Stenmark, 2009). The role of ubiquitylation events in protein trafficking extends beyond cargo modification. Various UBD-containing components of transport machineries undergo ubiquitylation (Klapisz *et al.*, 2002; Polo *et al.*, 2002; Marchese *et al.*, 2003; Shih *et al.*, 2003; McCullough *et al.*, 2004; Kim *et al.*, 2007a) through a process that requires functional UBDs, but the relevance of this modification is unclear. In yeast, only Vps27 and Hse1 have been shown to be ubiquitylated (Stringer and Piper, 2011; Ziv *et al.*, 2011; Starita *et al.*, 2012). In addition, Vps23 and the ESCRT-associated protein Bro1 (the functional equivalent of the mammalian Alix) interact with Rsp5 (Nikko and Andre, 2007; Ren *et al.*, 2007), suggesting that these proteins may also be ubiquitylated. ESCRT proteins also interact with deubiquitylating enzymes (DUBs; Clague and Urbe, 2006). For example, yeast Ubp2, which associates with Rsp5 and preferentially deubiquitylates proteins modified with K63Ub chains (Kee *et al.*, 2005), interacts indirectly with Hse1 (Ren *et al.*, 2007). Two mammalian DUBs—UBPY and AMSH—bind to several components of the ESCRT machinery. AMSH, which belongs to the JAMM-domain metalloprotease family of DUBs, specifically deubiquitylates K63Ub chains (McCullough *et al.*, 2004). In the absence of AMSH, both STAM (McCullough *et al.*, 2004; Sierra *et al.*, 2010) and Hrs (Sierra *et al.*, 2010) are strongly ubiquitylated. Thus, although the association of DUBs with the ESCRT machinery may allow the deubiquitylation of cargoes before their targeting into MVBs, it remains possible that some of these enzymes also play a role in Ub-based regulation of ESCRT complexes.

In the present study, we focus on MVB cargoes and their ubiquitylation and fate in yeast and mammalian cells unable and impaired, respectively, in the genesis of K63Ub chains. We also investigate the ubiquitylation status of all UBD-containing ESCRT proteins and the involvement of K63Ub chains in the homeostasis of MVBs in yeast.

RESULTS

MVB sorting of the yeast endosomal adapter Ear1 requires K63Ub chains

The yeast transmembrane proteins sorted into the ILVs for targeting to the vacuolar lumen are highly diverse. They include endocytic cargoes, vacuolar-resident enzymes, and several Rsp5 endosomal adaptors that facilitate substrate recognition and ubiquitylation at MVBs (Epple *et al.*, 2001; Katzmann *et al.*, 2001; Reggiori and Pelham, 2001; Stimpson *et al.*, 2006; Leon *et al.*, 2008). Some endocytic cargoes and vacuolar-resident enzymes have been shown to be modified by or require normal genesis of K63Ub chains for efficient MVB sorting (Stawiecka-Mirota *et al.*, 2007; Erpapazoglou *et al.*, 2008; Lauwers *et al.*, 2009; Paiva *et al.*, 2009; Stringer and Piper, 2011). We therefore wondered whether this was also the case for Rsp5 transmembrane adaptors. We investigated Ear1, a protein required for the ubiquitylation and targeting to MVBs of several cargoes (Leon *et al.*, 2008; Nikko and Pelham, 2009). We screened a collection of yeast strains genetically modified such that all the endogenous Ub genes were deleted, with Ub provided solely by plasmids encoding the wild-type (wt) or single Lys-to-Arg (KR) mutant form of Ub (with the exception of UbK48R, which does not support growth; Spence *et al.*, 1995). An Ear1-mCherry fusion protein was produced in these cells, and its ubiquitylation profile was assessed (Figure 1A). In cells expressing wt Ub, monoubiquitylated and polyubiquitylated species of Ear1-mCherry appeared as lower-mobility forms compared with the major unmodified fraction (Figure 1A, arrowhead; Leon *et al.*, 2008). This ubiquitylation profile remained unaltered in cells expressing all KR Ub mutants, except for the cells expressing UbK63R, which displayed an enrichment in the monoubiquitylated form of Ear1-mCherry (Figure 1A, arrow) at the expense of the polyubiquitylated species. We concluded that Ear1 was mostly ubiquitylated on one main target lysine, which receives short K63Ub chains.[1] We then investigated the subcellular distribution of Ear1-mCherry by fluorescence microscopy in the same set of strains. In cells expressing wt Ub, Ear1-mCherry was targeted to the vacuolar lumen (Figure 1B), consistent with the sorting of this protein into ILVs. A similar distribution profile was observed in almost all the strains expressing mutant UbKR forms. By contrast, the production of UbK63R as the sole source of Ub led to the accumulation of Ear1-mCherry at the vacuolar membrane, revealing a defect in ILVs sorting (Odorizzi *et al.*, 1998).

Thus the correct trafficking of Ear1 to the vacuole requires K63Ub chains, with no other type of Ub chain playing a major role in this process.

Proteins with K63Ub chains accumulate in the class E compartment

We then investigated the extent to which K63Ub chain formation was a feature common to MVB cargoes. To assess an eventual enrichment of K63Ub chains in yeast endosomes, we performed an immunofluorescence (IF) analysis using an anti-K63Ub antibody (Newton *et al.*, 2008). No specific cellular compartment was labeled by the antibody in cells expressing the wt or the K63RUb construct (Figure 2A). We repeated the same experiment in strains lacking the ESCRT-I protein Vps23. Mutants lacking any of the ESCRT subunits display an aberrant endosomal structure in close proximity to the vacuole, referred as the class E compartment (Raymond *et al.*, 1992;

[1]In cells depleted of K63Ub chains, Ear1-mCherry displayed a few bands in addition to the main monoubiquitylated form, indicating either multi-monoubiquitylation or modification by other types of Ub chains, as observed for the MVB cargo Sna3 (Stawiecka-Mirota *et al.*, 2007).

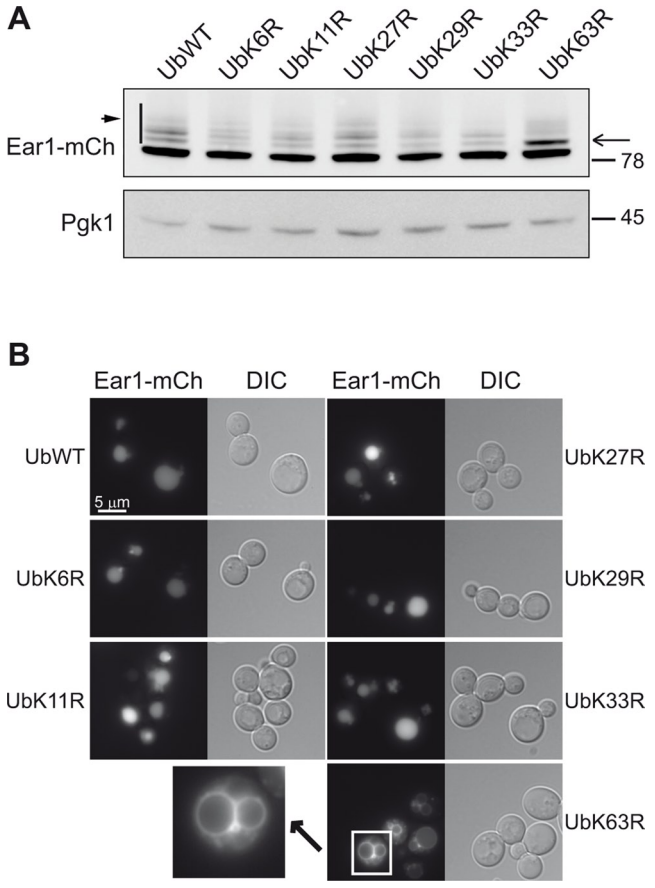

FIGURE 1: K63Ub chains are required for efficient sorting to yeast MVBs. SUB cells genetically modified to express only plasmid-encoded wt or single-KR-mutant Ub were transformed with a plasmid encoding Ear1-mCherry (mCh) under the control of the *GPD1* promoter. (A) Ear1-mCherry ubiquitylation profile. Total protein extracts separated by SDS–PAGE were immunoblotted with an anti-DsRed antibody. The arrow and arrowhead indicate the monoubiquitylated and polyubiquitylated forms of Ear1-mCherry, respectively. The anti-Pgk1 blot serves as a loading control. (B) Ear1-mCherry sorting to the MVB pathway was assessed by fluorescence microscopy.

Coonrod and Stevens, 2010). In ESCRT mutants, ubiquitylated cargo proteins accumulate in the class E compartment and at the vacuolar membrane due to the lack of sorting into ILVs (Katzmann *et al.*, 2001), as illustrated by fluorescence microscopy in Figure 2B for the siderophore transporter Sit1–green fluorescent protein (GFP) under conditions in which it is directly targeted from the Golgi to the MVB pathway (Erpapazoglou *et al.*, 2008). In addition, transporters trapped in the class E compartment, coming from either the plasma membrane or the Golgi apparatus, are known to recycle back to the plasma membrane (Bugnicourt *et al.*, 2004; Erpapazoglou *et al.*, 2008; Figure 2B). The class E compartment, evidenced by the accumulation of the MVB cargo GFP-Phm5 (Figure 2C), was the only cellular structure strongly labeled with the anti-K63Ub antibody in the *vps23*Δ mutant. This labeling was specific, and it was absent in *vps23*Δ cells expressing UbK63R as the sole source of Ub. The class compartment E was also uniformly labeled in *vps23*Δ cells that do not express GFP-Phm5 (Figure 2D). The vacuolar membrane (arrowhead) or the plasma membrane (arrow) was also specifically labeled in some *vps23*Δ cells. No labeling of these structures nor of the class E compartment was observed with an antibody directed against K48Ub chains, which leads to diffuse cytoplasmic and some nuclear staining (Figure 2D).

As a consequence of higher steady-state levels of transporters at the plasma membrane, *vps* class E mutants are more sensitive to the toxic compounds imported by some of these transporters (Forsberg *et al.*, 2001; Bugnicourt *et al.*, 2004; Ren *et al.*, 2007; Ruotolo *et al.*, 2008). Indeed, *vps23*Δ cells were very sensitive to 5-fluorouracil (5-FU), transported by the uracil permease Fur4, as previously reported (Bugnicourt *et al.*, 2004), and were also sensitive to ethionine, canavanine, and cadmium, imported by the methionine, arginine, and manganese transporters Mup1, Can1, and Smf1 (Grenson *et al.*, 1966; Isnard *et al.*, 1996; Liu *et al.*, 1997), respectively (Figure 2E). Cells unable to generate K63Ub chains had identical phenotypes, although in this case the presence of larger numbers of transporters at the plasma membrane may result from both an MVB sorting defect (Figure 1B) and slower endocytosis (Galan and Haguenauer-Tsapis, 1997).

Our data demonstrate that yeast late endosomal compartments are enriched in proteins carrying K63Ub chains, consistent with observations that several MVB substrates, such as endocytic and biosynthetic cargoes, harbor this modification, as do Rsp5 adapters (Galan and Haguenauer-Tsapis, 1997; Springael *et al.*, 1999; Kim *et al.*, 2007b; Stawiecka-Mirota *et al.*, 2007; Erpapazoglou *et al.*, 2008; Lauwers *et al.*, 2009; Paiva *et al.*, 2009; Figure 1), and are sorted to MVBs at this location. The observed staining however, might be also due to the recognition of additional proteins (see later discussion).

K63Ub chains are conjugated to the melanosomal protein MART-1 and are required for its sorting into MVBs

Several yeast MVB cargoes are known to require the synthesis of K63Ub chains for correct transport (Erpapazoglou *et al.*, 2008; Lauwers *et al.*, 2009; Stringer and Piper, 2011). However, no examples have been described in mammalian cells, despite both the high degree of conservation of the MVB sorting machinery and the presence of this type of modification on a large number of plasma membrane proteins during their endocytosis (Geetha *et al.*, 2005; Duncan *et al.*, 2006; Huang *et al.*, 2006; Kamsteeg *et al.*, 2006; Li *et al.*, 2008; Vina-Vilaseca and Sorkin, 2010; Sorrentino *et al.*, 2011).

We therefore decided to analyze the role of K63Ub chains in the modification and trafficking of a particular mammalian MVB cargo, MART-1/MelanA. MART-1 is an integral membrane protein involved in melanosome maturation (Giordano *et al.*, 2011). It passes through the Golgi compartment, the principal site at which it is found (De Maziere *et al.*, 2002), before being targeted to melanosomes via the MVB pathway (Levy *et al.*, 2005). This protein interacts with two human Rsp5 homologues, Nedd4 and Itch. It is ubiquitylated and undergoes Ub-dependent MVB sorting (Levy *et al.*, 2005; Giordano *et al.*, 2011). Endogenous MART-1 was thus immunoprecipitated from cell extracts in denaturing conditions. The same high–molecular weight species of MART-1 detected with the anti-MART-1 antibody (Figure 3A, panel 1) were also detected with both anti-Ub (panel 2) and anti-K63Ub (panel 3) antibodies, but no signal was observed with an antibody directed against K48Ub chains, which massively detects ubiquitylated proteins in total extracts (panel 4). These ubiquitylated forms of MART-1 contained two, three, or four Ub moieties (Figure 3A, arrows), demonstrating that MART-1 is polyubiquitylated, rather than multi-monoubiquitylated, and modified by short K63Ub chains. These findings are consistent with the observation that, like Rsp5, both Nedd4 and Itch principally mediate the synthesis of K63Ub chains in vitro (Kim and Huibregtse, 2009).

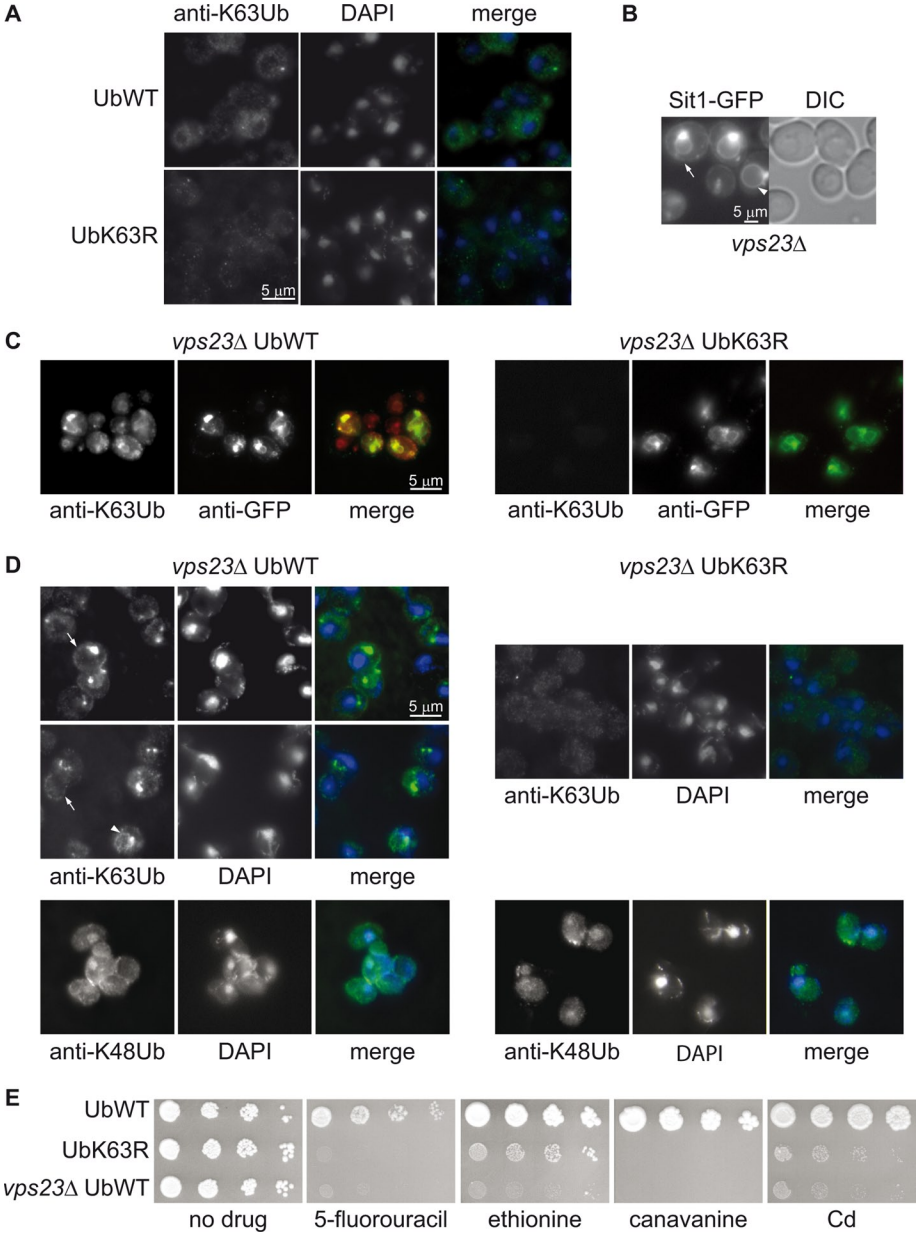

FIGURE 2: K63-linked chain-modified proteins accumulate in the class E compartment. (A) Yeast cells expressing plasmid-encoded wt or K63R Ub as sole source of Ub were analyzed by IF microscopy using an anti-K63Ub antibody. No specific labeling of any cellular structure was observed. (B) Localization of the MVB cargo Sit1-GFP in *vps23*Δ cells by fluorescence microscopy. The arrow and arrowhead show the presence of Sit1-GFP at the plasma and vacuolar membrane, respectively. (C) *vps23*Δ cells expressing plasmid-encoded wt Ub or UbK63R as the sole source of Ub and producing GFP-Phm5 were analyzed by IF microscopy with anti-K63Ub and anti-GFP antibodies. (D) *vps23*Δ cells expressing plasmid-encoded wt Ub or UbK63R as the sole source of Ub were analyzed by IF microscopy with anti-K63Ub or anti-K48Ub antibodies, combined with DAPI staining. The anti-K63Ub antibody labeled specifically and homogeneously the class E compartment in all cells. The vacuolar membrane (arrowhead) or the plasma membrane (arrow) were sporadically stained. (E) Serial dilutions of liquid cultures of cells expressing wt Ub (SUB280 and *vps23*Δ) or UbK63R (SUB413) transformed with an empty *URA3* plasmid (pRS316) were grown in solid YNB medium supplemented with 2% glucose in the presence or absence of toxic plasma membrane transporter substrates at the following concentrations: 5 μg/ml 5-FU, 10 μg/ml ethionine, 0.5 μg /ml canavanine, and 5 μM cadmium.

We then carried out an IF analysis of HeLa cells transfected with a plasmid expressing MART-1. The anti-K63Ub antibody labeled small, dot-like structures in the nucleus, as previously described (Pinato *et al*., 2009), but the main signal was associated with punctate structures throughout the cytoplasm, many of which colocalized with anti–MART-1 antibody-positive endosomes (Figure 3, B–G). In contrast, no colocalization was evidenced between MART1 and structures stained with an anti-K48Ub antibody (Supplemental Figure S1). These data complement the biochemical evidence and reveal that MART-1 is linked with K63Ub chains (Figure 3A). They also indicate that, as in yeast, the late endosomal compartments are enriched in proteins bearing this type of modification.

We investigated the potential role of K63Ub chains in the sorting of MART-1 to ILVs. HeLa cells were cotransfected with plasmids encoding MART-1 and either wt Ub-GFP or UbK63R-GFP. The C-terminal GFP moiety of these Ub fusions is released by cellular DUB-mediated cleavage, making it possible to monitor the expression of the Ub construct used for transfection (Tsirigotis *et al*., 2001; Duncan *et al*., 2006; Boname *et al*., 2010). The overproduction of UbK63R-GFP partially inhibits K63-mediated ubiquitylation by endogenous Ub (Duncan *et al*., 2006). Ultrathin cryosections were subjected to double-immunogold labeling with antibodies against MART-1 and GFP. As expected, GFP labeling was not associated with membrane structures but was cytoplasmic (Figure 4, A and B, arrowheads). By contrast, MART-1 labeling was associated with membrane compartments and, more precisely, with MVBs and some of the vesicles in their vicinity (Figure 4, A and B, arrows). In cells expressing wt Ub, MART-1 was sorted principally into the ILVs, as previously shown (Giordano *et al*., 2011). In contrast, in UbK63R-expressing cells, a significant fraction of MART-1 was retained on the limiting membrane of the MVBs (34.5 vs. 16.5% in cells expressing wt Ub).

Thus the inhibition of K63Ub chain elongation leads to a partial block of MART-1 sorting into ILVs. The mammalian MVB cargo MART-1 is therefore partly dependent on K63Ub chains for targeting to the interior of the lysosome. The inhibition of MVB sorting was only partial, probably because of the remaining endogenous wt Ub, and because nonubiquitylated MART-1 mutant (MART-1$^{K1\text{-}6R}$) was nonetheless partially sorted to MVBs in HeLa cells, indicating the existence of an additional, Ub-independent pathway (Giordano *et al*., 2011).

The in-frame fusion of the cargo to Ub only partially rescues sorting into MVBs in cells lacking K63Ub chains

The simplest explanation for the MVB targeting defects observed in both yeast and mammalian cells when K63-linked Ub chain

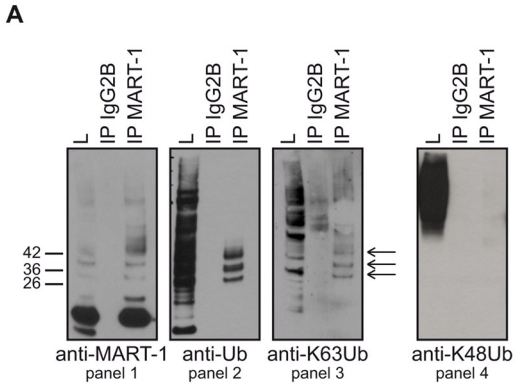

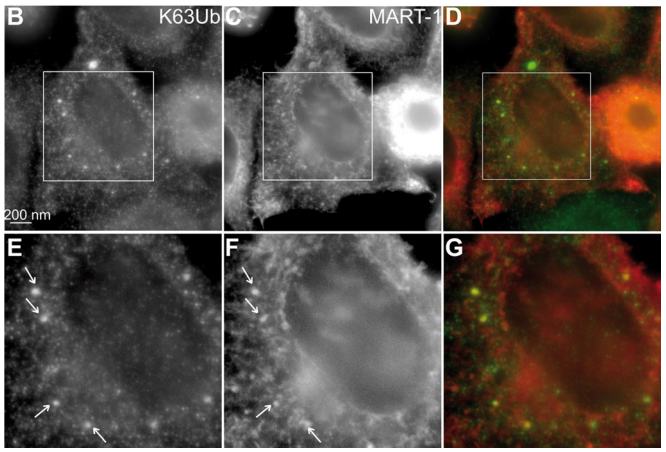

FIGURE 3: The human melanosomal protein MART-1 is modified by K63Ub chains. (A) Lysates from human melanocytic MNT-1 cells were immunoprecipitated with an anti-IgG2B (control) or anti-MART-1 antibody and immunoblotted with anti-MART-1, anti-Ub, anti-K63Ub, or anti-K48Ub antibodies. Arrows indicate ubiquitylated forms of MART-1 modified by K63Ub chains. (B–G) HeLa cells transfected with MART-1 were analyzed by IF microscopy with antibodies against MART-1 (C, F) and K63Ub chains (B, E). Overlays are shown in D and G. E–G correspond to a 1.8× magnification of the boxed areas in B–D, respectively.

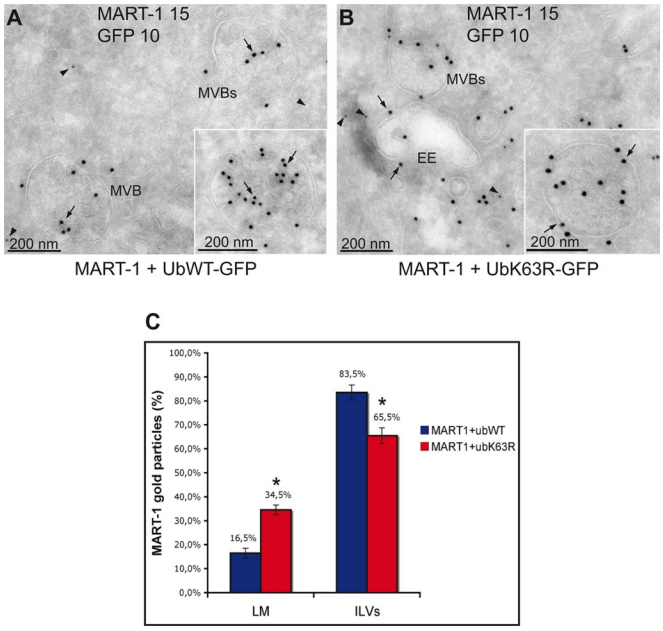

FIGURE 4: The inhibition of K63Ub chain formation impairs MART-1 endosomal sorting. (A, B) HeLa cells were transfected with plasmids encoding MART-1 and GFP-tagged wt Ub (Ub^{wt}-GFP) or UbK63R (Ub^{K63R}-GFP). Ultrathin cryosections were double immunogold labeled with anti–MART-1 (15-nm gold particles, arrow) and anti-GFP (10-nm gold particles, arrowhead) antibodies. (C) Quantification of the various sorting phenotypes of MART-1 as a percentage of gold particles per membrane compartment. EE, early endosomes; ILVs, intraluminal vesicles of the MVBs; LM, limiting membrane of the MVBs. Asterisk indicates deviation <0.05.

elongation is inhibited is that the cargo does not carry the optimal signal for recognition by the sorting machinery. Indeed, the UBDs of several ESCRT proteins have a higher affinity for K63Ub chains than for mono-Ub (Kulathu *et al.*, 2009; Ren and Hurley, 2010). Another, non–mutually exclusive possibility is that the sorting defects in cells depleted of K63Ub chains are caused by the impaired modification of other proteins, such as those of the sorting machinery itself.

The in-frame fusion of a single Ub to a nonubiquitylatable (KR) cargo has been shown to restore MVB sorting in yeast (Reggiori and Pelham, 2001; Urbanowski and Piper, 2001). If K63Ub chains are involved in regulating the MVB sorting machinery, then the in-frame fusion of Ub to a nonubiquitylatable cargo should not restore MVB sorting in cells unable to achieve this type of modification. We thus analyzed Phm5, a polyphosphate phosphatase that is ubiquitylated on its Lys6 by Rsp5 and reaches the vacuole lumen via the MVB pathway (Reggiori and Pelham, 2001; Morvan *et al.*, 2004). As expected, the sorting of Phm5 to MVBs was dependent on K63Ub chains, as shown by the accumulation of this protein at the vacuolar membrane in cells expressing UbK63R as the sole source of Ub (Figure 5A). We investigated the fate of Ub-GFP-Phm5-K6R, in which the Ub tag (mutated in target lysines 29, 48, and 63) bypasses the requirement for Phm5 ubiquitylation for efficient MVB sorting (Reggiori and Pelham, 2001; Morvan *et al.*, 2004). Ub-GFP-Phm5-K6R was normally sorted into the vacuolar lumen in most cells expressing wt Ub (Figure 5, B and C). In the strain expressing UbK63R, however, >50% of the cells displayed vacuolar membrane staining. This observation suggested that the absence of K63Ub chains affects the MVB sorting machinery.

All yeast UBD-containing ESCRT proteins are ubiquitylated

The defect in the sorting of Ub-GFP-Phm5-K6R to MVBs in cells unable to synthesize K63Ub chains and the frequent ubiquitylation of proteins carrying UBDs led us to investigate the ubiquitylation status of UBD-containing yeast ESCRT subunits and that of the ESCRT-associated Bro1 (Figure 6A), which has been reported to interact with Rsp5 (Nikko and Andre, 2007). We therefore assessed ESCRT ubiquitylation in wt cells, in a hypomorphic *rsp5* mutant (producing only 1/10 the normal amount of Rsp5; Hein *et al.*, 1995), and in *ubp2*Δ cells. We generated strains producing chromosomal-encoded, hemagglutinin (HA)-tagged ESCRT proteins in the wt and these two mutant strains. Total extracts of cells producing these HA-tagged ESCRT proteins together with hexahistidine (6His)-Ub were subjected to nickel-affinity chromatography, and the eluates were analyzed with an anti-HA antibody. More slowly migrating forms of Hse1-3xHA, 6xHA-Vps27, Vps36-3xHA, and Bro1-3xHA were detected in the eluates of wt cells (Figure 6B). These forms corresponded to ubiquitylated species, as they were not detected when untagged Ub was overproduced (Supplemental Figure S2A). Under the same experimental conditions, we detected no ubiquitylation of the ESCRT-I proteins Vps23-3xHA and Mvb12-3xHA (unpublished

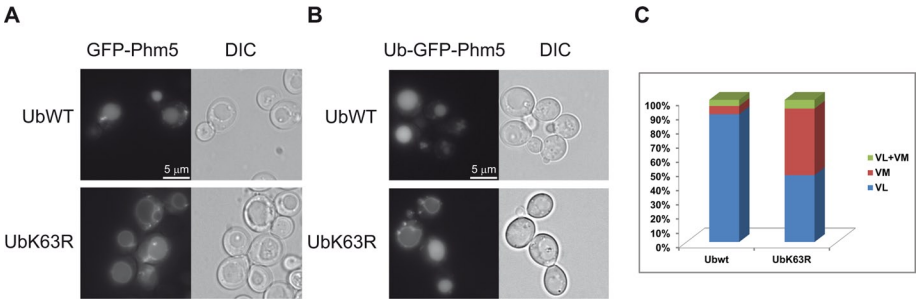

FIGURE 5: Ub fusion to the cargo only partially bypasses the MVB sorting defect in cells unable to synthesize K63Ub chains. (A) GFP-Phm5 was expressed in yeast expressing plasmid-encoded wt Ub (SUB280) or UbK63R as the sole source of Ub (SUB413). The efficiency of sorting to the vacuolar lumen was assessed by fluorescence microscopy. (B) Ub-GFP-Phm5-K6R was expressed in the same cells and observed by fluorescence microscopy. (C) Quantification of the various sorting phenotypes observed in B. The numbers indicate the percentage of the total cell population of 700 U. VL, vacuolar lumen; VM, vacuolar membrane. The heterogeneity of the observed sorting phenotypes is probably due to differences in the levels of Ub and cargo in individual cells.

data). The UBD-less, ESCRT-related AAA ATPase Vps4 was also not detected in the eluates (Supplemental Figure S2B).

With the exception of Bro1-3xHA, for which only a monoubiquitylated form was detected, all the proteins seemed to have multiple Ub moieties, consistent with multiubiquitylation or polyubiquitylation. The amounts of ubiquitylated species of Hse1-3xHA, 6xHA-Vps27, Vps36-3xHA, and Bro1-3xHA detected in the eluates of *rsp5* cells were much smaller (Figure 6B), suggesting that this ligase is involved in the modification of all these ESCRT proteins. The steady-state levels of the proteins were not significantly different in wt and *rsp5* cells, indicating that their degradation is not triggered by their ubiquitylation (Supplemental Figure S2C).

UBP2 deletion affected the ubiquitylation of a smaller number of ESCRT subunits than the rsp5 mutation. The ubiquitylation of 6xHA-Vps27 and Bro1-3xHA was unaffected, whereas clear increases were observed in both the amounts and the molecular weights of the ubiquitylated species for Hse1-3xHA and Vps36-3xHA (Figure 6B). Of interest, we also detected ubiquitylated species of Vps23-3xHA in this strain (Figure 6C). Given the specificity of Ubp2 for K63Ub chain disassembly (Kee *et al.*, 2006), Hse1, Vps23, and Vps36 may be targets of this type of modification.

The *ubp2*Δ cells do not display a difference in the ubiquitylation pattern of endocytic (Lam *et al.*, 2009) or biosynthetic cargoes (Ren *et al.*, 2007) and no impairment of the internalization step of endocytosis (Lam *et al.*, 2009). Ubp2 is required for a step occurring after Fur4 internalization, accounting for the hypersensitivity to 5-FU of *ubp2*Δ cells, possibly due to a defect in the sorting of this transporter into MVBs (Lam *et al.*, 2009). We investigated the possibility that, as described for *vps* class E mutants, *ubp2*Δ cells might be more generally susceptible than wild-type cells to toxic drugs imported by plasma membrane transporters. We found that *ubp2*Δ cells were hypersensitive to ethionine, canavanine, and cadmium (Figure 6D and Supplemental Figure S3), consistent with the typical MVB sorting defect already reported for these cells (Ren *et al.*, 2007). Our observation that some ESCRT proteins undergo Ubp2-dependent deubiquitylation provides a possible molecular explanation for the MVB-sorting phenotypes of *ubp2*Δ cells.

Inhibition of K63Ub chains formation leads to changes in the ultrastructure of MVBs

The observation that several ESCRT subunits undergo Rsp5-dependent ubiquitylation and Ubp2-dependent deubiquitylation and hence are possibly modified by K63Ub chains led us to investigate whether an inability to assemble or to disassemble these ubiquitin chains affected MVB ultrastructure. MVBs were not observed in ultrastructural studies of yeast until relatively recently (Luhtala and Odorizzi, 2004), as it is very difficult to capture these transient organelles on thin sections of wild-type cells. We therefore investigated MVB ultrastructure in cells carrying a thermosensitive variant of Vam3, a target soluble *N*-ethylmaleimide–sensitive factor attachment protein receptor protein essential for all vacuole fusion events (Darsow *et al.*, 1997). The *vam3-thermosensitive (vam-ts)* cells accumulated MVBs in large numbers, making it possible to perform statistical evaluations of morphology. To identify all the compartments of endosomal origin, we labeled the strains with Nanogold particles. These positively charged particles bind strongly to the negatively charged lipids present on the surface of yeast spheroplasts and are then internalized and, passing through the early (EE) and late (LE), endosomes, reach the vacuole (Prescianotto-Baschong and Riezman, 2002; Griffith and Reggiori, 2009). Thus spheroplasts were prepared from *vam3-ts* cells that were or were not able to assemble K63Ub chains or from cells with a *UBP2* deletion. They were then incubated with Nanogold particles at 4°C and transferred at the permissive temperature to allow internalization and labeling of EE and LE before finally being shifted at the restrictive temperature to accumulate late endosomal compartments before electron microscopic processing. As expected, the plasma membrane and vesicles, which are probably of endocytic origin, were labeled with the Nanogold particles in all three strains (Griffith and Reggiori, 2009; unpublished data). We observed at least one MVB per cell profile in cells expressing wt Ub (Figure 7, A, B, and J). These organelles, with a diameter between 160 and 200 nm, were occasionally found in clusters and contained well-defined ILVs. Nanogold particles also labeled two other compartments in these cells. The first consisted of clusters of vesicles and tubules (Figure 7C), probably corresponding to EEs (Wiederkehr *et al.*, 2000; Griffith and Reggiori, 2009) and hereafter referred to as type 1 EEs. The second labeled compartment consisted of large, tubular structures with gray contents, occasionally with a single internal membrane (Figure 7D). It was unclear whether these structures constituted a subclass of EEs or LE/MVBs or was a precursor of these organelles, but we nonetheless defined them as type 2 EEs, based on the rationale that the presence of luminal membranes is consistent with these structures being EEs in the process of becoming LE/MVBs.

MVBs were only rarely detected in the UbK63R-expressing strain (Figure 7J; 20% of the cell profiles displayed at least one MVB vs. 82% for cells with wt Ub). In this strain, the MVBs were often smaller (with a diameter of ~100 nm), with few ILVs, and their contents were less well defined than those of wt MVBs. We therefore called these structures "remnant MVBs" (Figure 7, E, F, F′, and J). Type 2 EEs were observed at a normal frequency in the UbK63R-expressing strain, whereas type 1 EEs were more frequent than in wild-type cells (50% of the cell profiles included at least one type 1 EE vs. 32% for cells expressing wt Ub), consistent with their accumulation (Figure 7, G, H, and J). These morphological observations revealed a severe impairment of MVB biogenesis in the absence of K63Ub

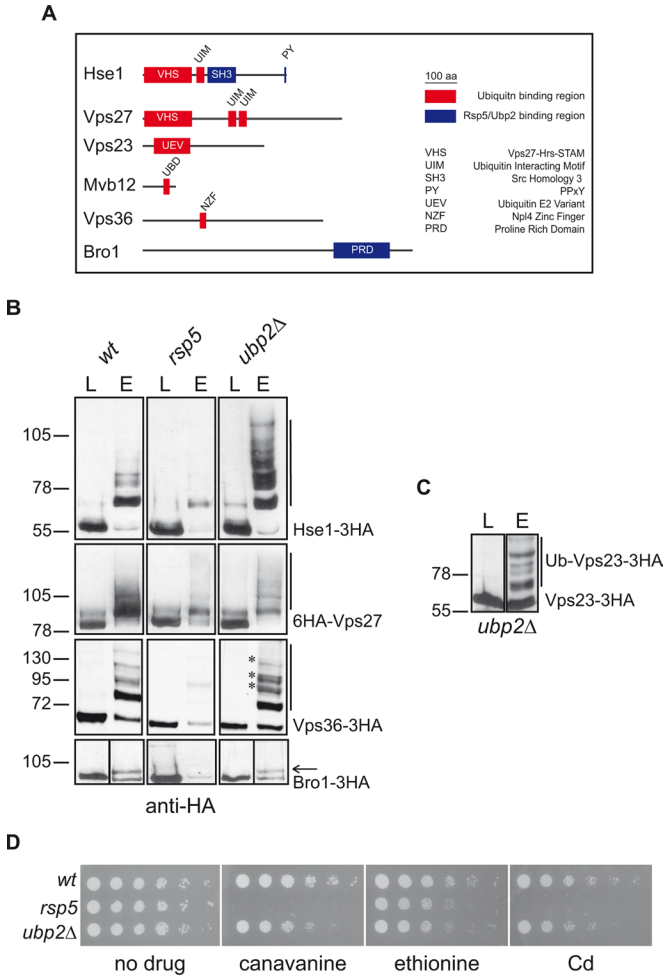

FIGURE 6: All UBD-containing ESCRT proteins are ubiquitylated. (A) Schematic representation of UBD-containing ESCRT proteins drawn to scale. (B) Cell lysates from wt, *rsp5*, or *ubp2*Δ strains (BY4741 genetic background) expressing Hse1-3xHA, 6xHA-Vps27, Vps36-3xHA, or Bro1-3xHA and overproducing 6His-Ub were passed through nickel columns. Lysates (L) and eluates (E) were subjected to SDS–PAGE and immunoblotted with an anti-HA antibody. Bars and arrows indicate the ubiquitylated forms of each protein. Asterisks indicate ubiquitylated forms of Vps36-3xHA specifically enriched in *ubp2*Δ cells. (C) The same experiment as in B was performed for *ubp2*Δ cells expressing Vps23-3xHA. (D) Serial dilutions of liquid cultures of 23344c (wt), 27038b (*npi1/rsp5*), and VA029 (*ubp2*Δ) cells were grown on solid YNB medium plus 2% glucose supplemented with uracil in the presence or absence of toxic plasma membrane transporter substrates, as described in Figure 2E.

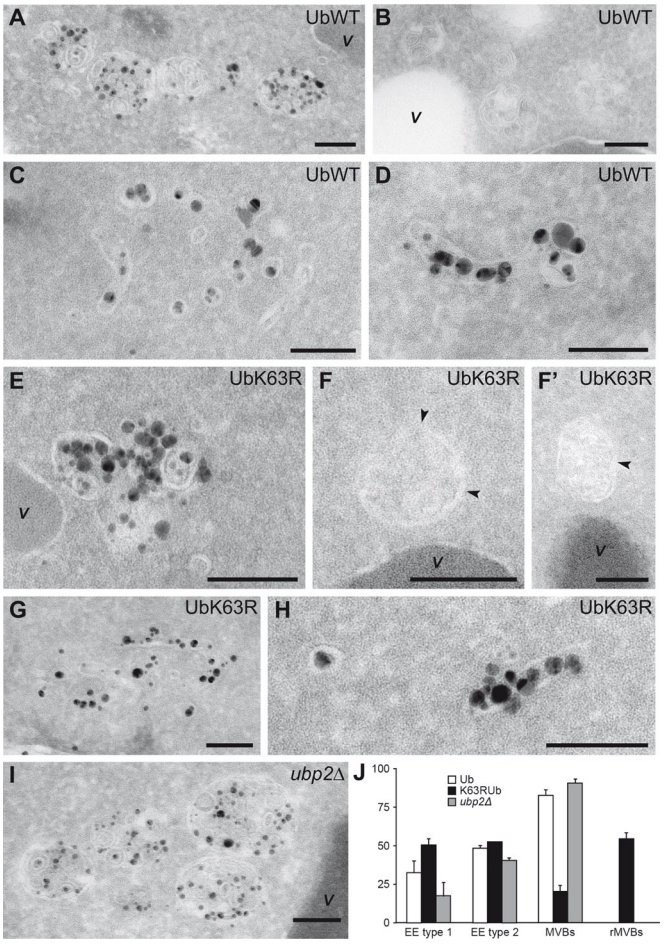

FIGURE 7: An inability to assemble or disassemble K63Ub chains affects MVBs biogenesis and ultrastructure. Ultrastructure of endosomal compartments in *vam3-ts* cells expressing wt or K63R Ub at the restrictive temperature. Nanogold particle uptake was assessed with spheroplasts obtained from RHT514, RHT515, and RHT516 cells before EM analysis. All the compartments accessible to the Nanogold particles were defined and subdivided into classes on the basis of morphological criteria (see *Materials and Methods*). (A) MVBs observed in RHT514 cells. (B) MVBs detected in preparations from the RH514 strain in which no silver enhancement reaction was performed, providing a clearer illustration of the morphological details of this organelle. (C) An example of a type1 EE from RHT514 cells. (D) The ultrastructure of a type 2 EE on sections from the RH514 strain. (E) A remnant MVB observed in the RHT515 mutant. (F, F') Remnant MVBs from a preparation in which no silver enhancement reaction was performed. (G) An example of a type1 EE detected in RHT515 cells. (H) A type 2 EE in the RH515 mutant. (I) MVBs observed in the *ubp2*Δ *vam3ts* mutant. (J) Statistical evaluation of the EM preparations. MVBs, type 1 and type 2 EEs, and remnant MVBs (rMVBs) were counted in 100 randomly chosen cell profiles in two independent experiments. Error bars represent the standard deviations, which were also used for a *t* test, confirming the statistical significance of the data ($p < 0.05$). Bar, 100 nm.

chains, possibly due to the impairment of EE maturation to generate LE/MVBs caused by a defect in ILV formation and/or in the homotypic fusion of endosomal compartments (Markgraf *et al.*, 2009).

vam3-ts ubp2Δ knockout cells had MVBs of normal size and morphology, which occasionally formed clusters (Figure 7, I and J). However, there were many more MVBs per cell profile than in cells expressing *UBP2* (3.15 ± 0.21 MVBs/cell profile vs. 2.12 ± 0.15 and 0.23 ± 0.10 in wt and UbK63R-expressing cells, respectively), suggesting a high rate of MVB formation in this strain background. Furthermore, type 1 EEs were more rarely detected in the *ubp2Δ* deletant, whereas type 2 EEs were not (Figure 7J; 17% of the cell profiles displayed at least one type 1 EE vs. 32% in cells expressing *UBP2*), consistent with a model in which the persistent presence of K63Ub chains on endosomal membranes increases the rate of transformation into MVBs.

DISCUSSION

We found that the Rsp5 adapter and MVB cargo Ear1 was mainly modified by K63Ub chains, thus extending the list of yeast cargoes

shown to display this type of ubiquitylation (Stawiecka-Mirota *et al.*, 2007; Lauwers *et al.*, 2009). Modification by these Ub chains is probably widespread, because the abnormal endosomes that form in ESCRT mutants, in which MVB cargoes accumulate, are the main intracellular structures recognized by a specific anti-K63Ub chain antibody. A requirement of K63Ub chains for efficient MVB sorting is also a feature of the human melanosomal MVB cargo MART-1, and endosomes are also the main structures immunolabeled with anti-K63Ub antibodies in human cells (Figure 3; Argenzio *et al.*, 2011; Giordano *et al.*, 2011).

The presence of K63Ub chains on yeast and human MVB cargoes, together with the MVB sorting defect in cells unable to assemble K63Ub chains, suggests that these chains provide a better sorting signal than monoubiquitylation. This could rely on an improved affinity of several ESCRT proteins for this modification. In general, UBDs bind mono-Ub with low affinity (Hicke *et al.*, 2005). K63Ub chains have a linear conformation in which the Ile-44–based hydrophobic patch on the surface of the Ub is highly accessible (Varadan *et al.*, 2004; Komander *et al.*, 2009). Vps27/Hrs and Hse1/STAM—the subunits of the ESCRT-0 complex—carry tandem UBDs, and they may therefore recognize several ubiquitin molecules in the context of a K63Ub chain. Consistent with this possibility, the STAM VHS domain binds K63-Ub_4 with a higher affinity than mono-Ub (Ren and Hurley, 2010), and the linear conformation of K63-Ub_2 was suggested to allow the first Ub moiety to interact with the VHS domain and the second with the UIM domain of STAM (Lange *et al.*, 2010). Finally, the NZF domain of Vps36—a component of the ESCRT-II complex—interacts with K63-Ub_2 with an affinity in the nanomolar range (Kulathu *et al.*, 2009).

Many UBD-containing proteins, including several human ESCRT proteins and the yeast Vps27 protein, have been shown to undergo ubiquitylation (Marchese *et al.*, 2003; McCullough *et al.*, 2004; Hurley *et al.*, 2006; Kim *et al.*, 2007a; Stringer and Piper, 2011). We found that all yeast UBD-containing ESCRT proteins underwent Rsp5-dependent ubiquitylation and that deubiquitylation of at least three of these proteins was mediated by Ubp2. The assembly and disassembly of K63Ub chains by Rsp5 and Ubp2, respectively, suggest that these proteins are likely modified by this type of Ub chain. Hence, the K63Ub chain staining of the class E compartment in *vps23*Δ cells could also possibly include the recognition of ESCRT proteins, known to accumulate together with cargoes in class E mutants (Katzmann *et al.*, 2001). The observations that STAM interacts with AMSH (Tanaka *et al.*, 1999; McCullough *et al.*, 2004), a DUB specifically involved in K63Ub chain disassembly (McCullough *et al.*, 2004), and that ubiquitylated forms of both STAM and Hrs accumulate in $AMSH^{-/-}$ cells (McCullough *et al.*, 2004; Sierra *et al.*, 2010) suggest that ESCRT proteins may also be modified by K63Ub chains in mammals.

UBD-dependent ubiquitylation of several UBD-containing proteins, occurring outside the UBD domain (Oldham *et al.*, 2002), was most generally presented as monoubiquitylation (Klapisz *et al.*, 2002; Polo *et al.*, 2002; reviewed in Hurley *et al.*, 2006). In vitro experiments with Eps15, a UIM-containing protein, suggested that this "coupled monoubiquitylation" might result from prior interaction between the UBD and an E3 that is itself ubiquitylated (Woelk *et al.*, 2006). This situation may also apply to ubiquitylated ESCRT proteins in yeast, because Rsp5 has been reported to be ubiquitylated (Ziv *et al.*, 2011), as confirmed here (Supplemental Figure S4A). The hypothesis of "coupled monoubiquitylation" must be modified, however, to take into account the fact that several yeast ESCRTs recognize specifically K63Ub chains, and according to our data, are most probably modified by these chains of Ub.

It has been suggested that the ubiquitylation of UBD-containing proteins leads to an intramolecular interaction between the UBD and Ub, potentially downregulating interaction *in trans* with ubiquitylated targets (Hoeller *et al.*, 2006; Hurley *et al.*, 2006). Our observation that several ESCRT proteins possibly undergo modification by K63Ub chains rather than monoubiquitylation suggests that modification by these Ub chains may increase the efficiency of release for the high-affinity interaction between K63Ub-modified cargoes and the UBD of ESCRT proteins.

Cells unable to assemble K63Ub chains do not accumulate class E compartment, as do mutants lacking any of the ESCRT proteins. However, they do display several ultrastructural abnormalities, that is, abnormal MVBs with a small diameter and few ILVs. The ubiquitylation of all UBD-containing ESCRT proteins in yeast—some likely with K63Ub chains—and the severe impairment of MVB biogenesis detected when this modification is inhibited suggest that ESCRT ubiquitylation may play a role in orchestrating the action of the various complexes and factors involved in the creation of this organelle and in the regulation of the MVB sorting process. However, future analysis of MVB biogenesis and sorting in cells having nonubiquitylable versions of one or likely several of the UBD-containing ESCRT proteins is required for checking rigorously the role played by ubiquitylation of these proteins via K63Ub chains.

Cells unable to assemble K63Ub chains displayed another morphological defect: an accumulation of type 1 EEs, which have been demonstrated to be bona fide EEs (Wiederkehr *et al.*, 2000), suggesting a defect in fusion at endosomes. It has been proposed that this process involves the tethering class C core vacuole/endosome tethering (CORVET) complex (Markgraf *et al.*, 2009). This complex includes three proteins—Vps8, Vps11, and Vps18—all of which carry a RING zinc finger domain (Nickerson *et al.*, 2009). This domain is common to many ubiquitin ligases (Weissman, 2001). Of interest, the RING domain of human Vps18 has been reported to display E3 ligase activity in vitro (Yogosawa *et al.*, 2005, 2006). Further studies are required to determine whether ubiquitylation events, possibly involving K63Ub chains, regulate the function of the CORVET complex in vivo. This hypothesis is converging with *Caenorhabditis elegans* data, in which K63Ub chains synthesized by the specific Uev1-Ubc13 E2 enzyme are required for early endosomes sorting of the α-amino-3-hydroxy-5-methyl-4-isoxazolepropionic acid–type glutamate receptor subunit GLR-1 (Kramer *et al.*, 2010).

Some MVB cargoes were found to display deficient MVB sorting in *ubp2*Δ cells (Lam *et al.*, 2009; Ren *et al.*, 2007). Consistent with a general MVB sorting defect, we confirmed that, like cells unable to synthesize K63Ub chains, the *ubp2*Δ strain was hypersensitive to many drugs imported by plasma membrane transporters, a hallmark of mutants with ESCRT protein defects (Bugnicourt *et al.*, 2004; Ruotolo *et al.*, 2008). Hence, Ubp2-dependent ESCRT deubiquitylation seems to be required for the regulation of MVB biogenesis and sorting. Similar to the situation we observed in yeast, AMSH was required for the correct trafficking, MVB sorting, and degradation of several receptors, including CXCR4 and EGFR (Ma *et al.*, 2007; Sierra *et al.*, 2010). Moreover, the *Schizosaccharomyces pombe* homologue of AMSH has been classified as a class E Vps protein (Iwaki *et al.*, 2007), and the plant homologue AMSH3 is required for normal vacuole biogenesis (Isono *et al.*, 2010).

During viral infection, Nedd4-like E3s and the ESCRT machinery are hijacked for the purposes of viral budding, through the ubiquitylation of Gag-related proteins in particular (Martin-Serrano, 2007). The simple ubiquitylation of Gag is not sufficient for this process, and the synthesis of K63Ub chains has been shown to be critical for Ub-mediated viral release, although the origin of

this defect remains to be defined (Strack *et al*., 2002; Weiss *et al*., 2010). Our data shed new light on these observations. We established that ubiquitylation dynamics, particularly as concerns the assembly and disassembly of K63Ub chains, regulates MVB sorting, and that several components of the ESCRT machinery are likely modified by these Ub chains. The coordination of these two events may be essential for the correct functioning of this crucial trafficking step. Future studies are required to determine the precise role played by ESCRT ubiquitylation/deubiquitylation during ILVs formation and to pinpoint the potential function of these modifications in the kinetics of ESCRT complex formation or in ESCRT interactions with protein or lipid partners.

MATERIALS AND METHODS

Yeast strains and plasmids

The *S. cerevisiae* strains in this study are listed in Table 1. With the exception of Vps27, all the C-terminally 3xHA-tagged proteins are functional, as shown by the levels of carboxypeptidase Y secretion into the medium and/or the sorting of a model MVB cargo, the siderophore transporter Sit1 (unpublished data). The insertion of the 6xHA tag at the N-terminus of Vps27 did not affect the function of this protein. Cells were grown at 30°C in yeast extract/peptone/dextrose, yeast nitrogen base (YNB; Difco, Detroit, MI) plus 2% glucose and the required supplements, or synthetic complete (SC) medium (YNB, 2% glucose, and complete synthetic medium; Difco), lacking the appropriate nutrient for plasmid selection. $CuSO_4$ was added at a final concentration of 100 μM for the induction of plasmid-encoded Ub genes. Yeast sensitivity to toxic substrate analogues was assessed in SC–2% agar supplemented with 5 μg/ml 5-FU, 10 μg/ml ethionine, 0.5 μg/ml canavanine, or 5 or 10 μM $CdCl_2$ as indicated. *vps23Δ SIT1-GFP* cells were grown to mid-exponential phase on 2% raffinose synthetic medium. Galactose was added to the medium at a final concentration of 2%, and the cells were incubated for 1 h to induce the expression of Sit1-GFP.

The plasmids used in this study are listed in Table 2. The PCR product, which includes the 5′ untranslated region of *HSE1*, was inserted between the *Eco*RI and *Xho*I sites of pRS426 (Sikorski and Hieter, 1989), generating pRS426-HSE1-3xHA. We generated pRS316-VAM3ts by inserting the 2.4-kb *Sal*I/*Bam*HI fragment of pVAM3ts414 (Darsow *et al*., 1997) into pRS316 (Sikorski and Hieter, 1989).

Yeast cell extracts, Western blots, and antibodies

Total protein extracts were prepared by the NaOH/trichloroacetic acid (TCA) lysis technique (Volland *et al*., 1994). Proteins were separated by SDS–PAGE and transferred to nitrocellulose membranes. The primary antibodies used for immunoblotting were monoclonal anti-Pgk1 (clone 22CS; Invitrogen, Carlsbad, CA), monoclonal anti-HA (clone 12CA5; Santa Cruz Biotechnology, Santa Cruz, CA), polyclonal anti-DsRed (Clontech, Mountain View, CA), monoclonal anti-ubiquitin (P4D1) directly coupled to horseradish peroxidase (HRP; Santa Cruz Biotechnology), monoclonal anti–MART-1 (7c10; Abcam, Cambridge, MA), polyclonal anti–MART-1 (Ep1422Y; Abcam), polyclonal anti-Nedd4 (BD Biosciences, San Jose, CA), polyclonal anti-K63Ub (clone Apu3; Millipore, Billerica, MA), and polyclonal anti-K48Ub (clone Apu2; Millipore) antibodies. Primary antibodies were then detected by incubation with secondary antibodies conjugated to HRP (Sigma-Aldrich, St. Louis, MO). Immunoblotting images were acquired with either the LAS-4000 imaging system (Fujifilm, Tokyo, Japan) or the Amersham Hyperfilm ECL system (GE Healthcare, Chalfont, United Kingdom).

Immunoprecipitation of MART-1 and detection of ubiquitylated conjugates

MNT-1 cells were cultured and lysed as previously described (Giordano *et al*. 2009, 2011). Cell lysates were cleared by incubation for 1 h with IgG2b (CD9) antibody-linked beads at 4°C, with shaking. Endogenous MART-1 was immunoprecipitated by incubation with 1 μg of anti–MART-1 antibody bound to protein G–agarose beads (Invitrogen) for 3 h at 4°C. IgG2b (CD9)-beads were used as a control. The beads were washed six times in cold lysis buffer, and the immunoprecipitates were eluted in sample buffer (Invitrogen), denatured by boiling, and separated by electrophoresis in Nu-PAGE 4–12% Bis-Tris gels (Invitrogen) for immunoblot analysis.

Immunofluorescence microscopy and immuno–electron microscopy in HeLa cells

HeLa cells were cultured as previously described (Giordano *et al*., 2009). For IF, cells were grown on coverslips and fixed in 4% paraformaldehyde (PFA) in phosphate-buffered saline (PBS). IF microscopy was carried out as previously described (Giordano *et al*. 2009), with monoclonal anti–MART-1 or polyclonal anti-K63Ub antibodies, followed by incubation with Alexa 568–conjugated anti-mouse or Alexa 488–conjugated anti-rabbit antibodies (Molecular Probes, Eugene, OR), respectively. For immuno–electron microscopy, HeLa cells were fixed by incubation with a mixture of 2% PFA and 0.2% glutaraldehyde in 0.1 M phosphate buffer and processed for ultracryomicrotomy and immunogold labeling (Slot and Geuze, 2007). Ultrathin cryosections were double immunogold labeled with polyclonal anti-GFP (Molecular Probes) and monoclonal anti–MART-1 antibodies and protein A coupled to 10- or 15-nm gold particles (Cell Microscopy Center, University Medical Center Utrecht, Utrecht, Netherlands), as indicated. Sections were observed under a CM120 electron microscope (FEI, Eindhoven, Netherlands) equipped with a KeenView camera (Olympus Soft Imaging System, Münster, Germany). For the quantification of MART-1 labeling, 200 gold particles were counted in randomly selected endosomal compartments in each of two separate experiments. Data are presented as the mean ± SD, with analysis by Student's *t* test ($p < 0.05$).

Purification of hexahistidine-Ub protein conjugates

The 6His-tagged ubiquitylated proteins were purified from 100 OD_{600} equivalents of exponentially growing yeast cells expressing 6His-tagged Ub as previously described (Ziv *et al*., 2011). 6His-Ub conjugates were retained on nickel–nitrilotriacetic acid Sepharose beads (Qiagen, Hilden, Germany), eluted in the presence of 500 mM imidazole, and precipitated with 10% TCA (eluate [E]). Lysates (L) correspond to 1/50 of the sample before incubation with the beads, precipitated with TCA. Lysate and eluate samples were analyzed by SDS–PAGE, followed by immunoblotting.

IF of yeast cells

This analysis was performed as previously described (Belgareh-Touze *et al*., 2002). We fixed 30–50 OD_{600} equivalents of cells grown to mid-exponential phase by incubation for 1 h with 3.7% formaldehyde at room temperature. Cells were treated with 100 mM Tris-HCl, pH 9.4, and 10 mM dithiothreitol for 8 min and converted into spheroplasts by incubation with Zymolyase 20T (Seikagaku, Tokyo, Japan; 0.2 mg/ml in 1.2 M sorbitol/20 mM potassium phosphate buffer, pH 7.4). Spheroplasts were spotted onto polylysine-coated slides and permeabilized with 0.1% or 0.5% Triton X-100 in PBS (50 mM potassium phosphate, pH 7.5, 150 mM NaCl). For Figure 2C, cells were incubated with monoclonal anti-GFP (clones 7.1

Strain	Genotype	Source/ reference
23344c	*Mata ura3* (Σ*1278b* genetic background)	Bruno André Université LIbre de Bruxelles, Belgium
27038a	*Mata ura3 npi1* (Σ*1278b* genetic background; mutation in *RSP5* promoter)	Bruno André (Hein *et al.*, 1995)
VA029	*Mata ura3 ubp2Δ::KanMX6* (Σ*1278b* genetic background)	Bruno André
BY4741 (WT)	*Mata his3Δ1 leu2Δ0 met15Δ0 ura3Δ0*	EUROSCARF
RHT 499	*Matα his3Δ1 leu2Δ0 met15Δ0 ura3Δ0 promKanMX4-RSP5*	Bruno André (Erpapazoglou *et al.*, 2008)
RHT 500	*Mata his3Δ1 leu2Δ0 met15Δ0 ura3Δ0 ubp2Δ::KanMX6*	EUROSCARF
RHT 501 (HSE1-3xHA)	*Mata his3Δ1 leu2Δ0 met15Δ0 ura3Δ0 HSE1-3HA::HIS3MX6*	This study
RHT 502 (6xHA-VPS27)	*Mata his3Δ1 leu2Δ0 met15Δ0 ura3Δ0 6xHA-VPS27*	This study
RHT503 (VPS36-3xHA)	*Mata his3Δ1 leu2Δ0 met15Δ0 ura3Δ0 VPS36-3xHA::HIS3MX6*	This study
RHT504 (BRO1-3xHA)	*Mata his3Δ1 leu2Δ0 met15Δ0 ura3Δ0 BRO1-3xHA::HIS3MX6*	This study
RHT505 (HSE1-3xHA/ rps5)	*Matα his3Δ1 leu2Δ0 met15Δ0 ura3Δ0 promKanMX4-RSP5 HSE1-3xH::HIS3MX6*	This study
RHT506 (6xHA-VPS27/ rsp5)	*Matα his3Δ1 leu2Δ0 met15Δ0 ura3Δ0 promKanMX4-RSP5 6xHA-VPS27*	This study
RHT507 (VPS36-3xHA/ rps5)	*Matα his3Δ1 leu2Δ0 met15Δ0 ura3Δ0 promKanMX4-RSP5 VPS36-3xHA::HIS3MX6*	This study
RHT508 (BRO1-3xHA/ rsp5)	*Matα his3Δ1 leu2Δ0 met15Δ0 ura3Δ0 promKanMX4-RSP5 BRO1-3xHA::HIS3MX6*	This study
RHT509 (HSE1-3xHA/ ubp2Δ)	*Mata his3Δ1 leu2Δ0 met15Δ0 ura3Δ0 ubp2Δ::KanMX6 HSE1-3xHA::HIS3MX6*	This study
RHT510 (6xHA-VPS27/ ubp2Δ)	*Mata his3Δ1 leu2Δ0 met15Δ0 ura3Δ0 ubp2::KanMX6 6xHA-VPS27*	This study
RHT511 (VPS23-3xHA/ ubp2Δ)	*Mata his3Δ1 leu2Δ0 met15Δ0 ura3Δ0 ubp2Δ::KanMX6 VPS23-3xHA::HIS3MX6*	This study
RHT512 (VPS36-3xHA/ ubp2Δ)	*Mata his3Δ1 leu2Δ0 met15Δ0 ura3Δ0 ubp2Δ::KanMX6 VPS36-3xHA::HIS3MX6*	This study
RHT513 (BRO1-3xHA/ ubp2Δ)	*Mat a his3Δ1 leu2Δ0 met15Δ0 ura3Δ0 ubp2Δ::KanMX6 BRO1-3xHA::HIS3MX6*	This study
SUB280	*Mata ubi1-Δ1::TRP1 ubi2-Δ2:ura3, ubi3-Δub-2 ubi4-Δ2::LEU2 (pUB39-Ub) (pUB100) lys2-801 leu2-3112 ura3-52 his3-Δ200 trp1-1(am)*	Spence *et al.* (1995)
SUB413	*Mata ubi1-Δ1::TRP1 ubi2-Δ2:ura3, ubi3-Δub-2 ubi4-Δ2::LEU2 (pUB39-UbK63R) (pUB100) lys2-801 leu2-3112 ura3-52 his3-Δ200 trp1-1(am)*	Spence *et al.* (1995)
SUB515	*Mata ubi1-Δ1::TRP1 ubi2-Δ2:ura3, ubi3-Δub-2 ubi4-Δ2::LEU2 (pUB39-UbK6R) (pUB100) lys2-801 leu2-3112 ura3-52 his3-Δ200 trp1-1(am)*	Spence *et al.* (1995)
SUB516	*Mata ubi1-Δ1::TRP1 ubi2-Δ2:ura3, ubi3-Δub-2 ubi4-Δ2::LEU2 (pUB39-UbK11R) (pUB100) lys2-801 leu2-3112 ura3-52 his3-Δ200 trp1-1(am)*	Spence *et al.* (1995)
SUB517	*Mata ubi1-Δ1::TRP1 ubi2-Δ2:ura3, ubi3-Δub-2 ubi4-Δ2::LEU2 (pUB39-UbK27R) (pUB100) lys2-801 leu2-3112 ura3-52 his3-Δ200 trp1-1(am)*	Spence *et al.* (1995)
SUB518	*Mata ubi1-Δ1::TRP1 ubi2-Δ2:ura3, ubi3-Δub-2 ubi4-Δ2::LEU2 (pUB39-UbK29R) (pUB100) lys2-801 leu2-3112 ura3-52 his3-Δ200 trp1-1(am)*	Spence *et al.* (1995)
SUB519	*Mata ubi1-Δ1::TRP1 ubi2-Δ2:ura3, ubi3-Δub-2 ubi4-Δ2::LEU2 (pUB39-UbK33R) (pUB100) lys2-801 leu2-3112 ura3-52 his3-Δ200 trp1-1(am)*	Spence *et al.* (1995)
SUB280 vps23Δ	*Mata ubi1-Δ1::TRP1 ubi2-Δ2:ura3, ubi3-Δub-2 ubi4-Δ2::LEU2 (pUB39-Ub) (pUB100) lys2-801 leu2-3112 ura3-52 his3-Δ200 trp1-1(am) vps23Δ::KanMX6*	Helle Ulrich, London Research Institute, UK
SUB413 vps23Δ	*Mata ubi1-Δ1::TRP1 ubi2-Δ2:ura3 ubi3-Δub-2 ubi4-Δ2::LEU2 (pUB39-UbK63R) (pUB100) lys2-801 leu2-3112 ura3-52 his3-Δ200 trp1-1(am) vps23Δ::KanMX6*	Helle Ulrich
TDY2 vam3ts	*Mata ura3-52 leu2-3112 his3-Δ200 trp1-Δ901 lys2-801 suc2-Δ9 mel GAL vam3Δ::LEU2 + pVAM3ts414*	Darsow *et al.* (1997)
RHT516 (ubp2Δ vam3-ts)	*Mata ura3-52 leu2-3112 his3-Δ200 trp1-Δ901 lys2-801 suc2-Δ9 mel ubp2Δ::KanMX6 GAL vam3Δ::LEU2 + pVAM3ts414*	This study

TABLE 1: The *S. cerevisiae* strains used.

Continues

Strain	Genotype	Source/ reference	Strain	Genotype	Source/ reference
RHT514 (SUB280 vam3-ts)	*Mata ubi1-Δ1::TRP1 ubi2-Δ2:ura3, ubi3-Δub-2 ubi4-Δ2::LEU2 (pUB39-Ub) (pUB100) lys2-801 leu2-3112 ura3-52 his3-Δ200 trp1-1(am) vam3Δ::KanMX6 + pRS316-VAM3ts*	This study	*RHT515 (SUB413 vam3-ts)*	*Mata ubi1-Δ1::TRP1 ubi2-Δ2:ura3, ubi3-Δub-2 ubi4-Δ2::LEU2 (pUB39-UbK63R) (pUB100) lys2-801 leu2-3112 ura3-52 his3-Δ200 trp1-1(am) vam3Δ::KanMX6 + pRS316-VAM3ts*	This study

EUROSCARF, European *Saccharomyces cerevisiae* Archive for Functional Analysis, Institute for Molecular Biosciences, Johann Wolfgang Goethe-University Frankfurt, Frankfurt, Germany.

TABLE 1: The *S. cerevisiae* strains used. Continued

and 13.1; Roche Diagnostics, Mannheim, Germany) and polyclonal anti-K63Ub (diluted 1:20 or 1:40 in PBS/1% bovine serum albumin), followed by incubation with donkey anti–mouse immunoglobulin G (IgG) coupled to fluorescein isothiocyanate (FITC) and goat anti–rabbit IgG coupled to Texas red (diluted 1:500), respectively. For Figure 2D, cells were incubated with either anti-K63Ub or anti-K48Ub antibodies, followed by incubation with donkey anti–rabbit IgG coupled to FITC. All secondary antibodies were from Jackson ImmunoResearch Laboratories (West Grove, PA). Nuclei were stained with 0.2 ng/μl 4′,6-diamidino-2-phenylindole (DAPI). The slides were finally mounted in Citifluor (Citifluor, London, United Kingdom).

Plasmid	Characteristics, use	Reference
pRS316	*CEN, URA3* (Figure 2)	Sikorski and Hieter (1989)
pSL22	*GPD1, CEN, LEU2*; expression of Ear1-mCherry (Figure 1)	Leon *et al.* (2008)
pGFP-Phm5	*TPI1, CEN, URA3*; expression of GFP-Phm5 (Figures 2C and 5A)	Reggiori and Pelham (2001)
pUb-GFP-Phm5-K6R	*TPI1, CEN, URA3*; expression of Ub(K29,48,63R)-GFP-Phm5-K6R (Figure 5B)	Reggiori and Pelham (2001)
YEp352-HisUb	*CUP1, 2μ, URA3*; expression of 6His-Ub (Figure 6B)	Vitaliano-Prunier *et al.* (2008)
pVAM3ts414	*promVAM3, CEN, TRP1*; construction of strains *SUB280 vam3ts* and *SUB413 vam3ts*	Darsow *et al.* (1997)
pRS316-VAM3ts	*promVAM3, CEN, URA3* (Figure 7)	This study
pcDNA3-MART-1	Expression of MART-1 (Figures 3B and 4)	Levy *et al.* (2005)
pHR-SIN-CMVp-6His-wt Ub-GFP	Expression of 6His-wtUb-GFP (Figure 4)	Boname *et al.* (2010), Tsirigotis *et al.* (2001)
pHR-SIN-CMVp-6His-UbK63R-GFP	Expression of 6His-Ub-K63R-GFP (Figure 4)	Boname *et al.* (2010), Tsirigotis *et al.* (2001)
pSIT1-GFP	*GAL1, CEN, URA3*; expression of Sit1-GFP (Figure 2B)	Froissard *et al.* (2007)

TABLE 2: The plasmids used.

Fluorescence microscopy

Fluorescence microscopy in yeast was carried out with an Olympus BY61 microscope (Olympus, Tokyo, Japan) equipped with the following filter sets: FITC for GFP (Filter 41001 FITC, Exciter HQ480/40x, Dichroic Q505LP, Emitter HQ535/50 nm; Chroma Technology, Bellows Falls, VT), propidium iodide for mCherry (Filter 41005, Exciter HQ535/50x, Dichroic Q565LP, Emitter HQ645/75m), and DAPI (Filter 31013v2 DAPI, Exciter D365/40x, Dichroic 400DCLP). Cell contours were visualized with Nomarski optics. Images were acquired with a SPOT4.05 charge-coupled device camera (SPOT Imaging Solutions, Sterling Heights, MI).

Mammalian cells were examined with a Leica Microsystems DM-RXA2 three-dimensional (3D) deconvolution microscope (Leica, Nanterre, France) equipped with a piezo Z-drive and a 100×, 1.4 numerical aperture, PL-APO objective lens for optical sectioning (Physik Instrument, Pantin, France). Images are maximum-intensity *z*-projections of three 3D image stacks acquired using the MetaMorph software (MDS Analytical Technologies, Sunnyvale, CA) through a CoolSNAP HQ camera (Photometrics, Tucson, AZ).

Electron microscopy in yeast

Endosomal compartments were labeled with positively charged Nanogold particles, and ultrastructure analysis was carried out by electron microscopy (EM) as previously described (Griffith and Reggiori, 2009), but with the following modifications. The cells were grown and converted into spheroplasts at 24°C. The samples were incubated for 15 min in the presence of Nanogold particles (1.4-nm mean diameter; Nanoprobes, Stony Brook, NY) at 4°C and were then shifted to 24°C for 10 min and then 38°C for 40 min before processing and EM analysis. Cryosections were cut and placed in 0.6% uranyl acetate in 1% methyl cellulose/1.15 M sucrose in PHEM buffer (20 mM 1,4-piperazinediethanesulfonic acid, 50 mM 4-(2-hydroxyethyl)-1-piperazineethanesulfonic acid, pH 6.9, 20 mM ethylene glycol tetraacetic acid, 4 mM $MgCl_2$) before staining to enhance membrane contrast (Griffith *et al.*, 2008). The EM experiments were quantified by determining the relative number of defined organelles per cell section by analyzing 100 randomly chosen cell profiles from two independent experiments. All the

compartments accessible to Nanogold particles were defined and classified on the basis of morphological criteria as follows: type 1 EEs are clusters of vesicles and thin tubules; type 2 EEs are large, tubular structures with gray content that from time to time contain one internal membrane; MVBs are circular structures with a mean diameter of 200 nm and with a lumen filled with vesicles; and remnant MVBs are circular structures with a mean diameter of 100 nm and with a less well defined content that can display the presence of few internal vesicles.

ACKNOWLEDGMENTS

We thank Helle Ulrich for providing the SUB413 *vps23Δ* strain of yeast, Dan Finley for the collection of SUB yeast strains, Robert Piper for the Vps36$^{\Delta NZF}$ mutant, Paul Lehner for the Ub-GFP plasmids, and Janice Griffith for technical assistance. We thank Ahmed El Marjou for his help in technical issues. We are grateful to Naïma Belgareh-Touzé for her continual assistance during this work. We thank Alex Edelman and associates for editorial assistance. R.H.T. is supported by the Centre National de la Recherche Scientifique, Paris 7–Université Paris-Diderot, and by grants from the Association pour la Recherche contre le Cancer (Grant 3298), the Ligue Nationale Contre le Cancer (Comité de Paris, grant RS09/75-26), the European Commission 6th Framework Program (Role of Ubiquitin and Ubiquitin-like Modifiers in Cellular Regulation [RUBICON]), and the Marie Curie UBIREGULATORS network. G.R. is supported by the Institut Curie, Centre National de la Recherche Scientifique and Association pour la Recherche contre le Cancer. F.R. is supported by the Netherlands Organization for Health Research and Development (ZonMW-VIDI-917.76.329) and by the Netherlands Organization for Scientific Research (Chemical Sciences, ECHO grant-700.59.003). Z.E. held fellowships from the UBIREGULATORS and RUBICON networks. M.P. and M.D. held fellowships from the RUBICON network. F.G. held a fellowship from the Fondation pour la Recherche Médicale.

REFERENCES

Argenzio E, Bange T, Oldrini B, Bianchi F, Peesari R, Mari S, Di Fiore PP, Mann M, Polo S (2011). Proteomic snapshot of the EGF-induced ubiquitin network. Mol Syst Biol 7, 462.

Belgareh-Touze N, Avaro S, Rouille Y, Hoflack B, Haguenauer-Tsapis R (2002). Yeast Vps55p, a functional homolog of human obesity receptor gene-related protein, is involved in late endosome to vacuole trafficking. Mol Biol Cell 13, 1694–1708.

Belgareh-Touze N, Leon S, Erpapazoglou Z, Stawiecka-Mirota M, Urban-Grimal D, Haguenauer-Tsapis R (2008). Versatile role of the yeast ubiquitin ligase Rsp5p in intracellular trafficking. Biochem Soc Trans 36, 791–796.

Boname JM, Thomas M, Stagg HR, Xu P, Peng J, Lehner PJ (2010). Efficient internalization of MHC I requires lysine-11 and lysine-63 mixed linkage polyubiquitin chains. Traffic 11, 210–220.

Bugnicourt A, Froissard M, Sereti K, Ulrich HD, Haguenauer-Tsapis R, Galan JM (2004). Antagonistic roles of ESCRT and Vps class C/HOPS complexes in the recycling of yeast membrane proteins. Mol Biol Cell 15, 4203–4214.

Clague MJ, Urbe S (2006). Endocytosis: the DUB version. Trends Cell Biol 16, 551–559.

Coonrod EM, Stevens TH (2010). The yeast vps class E mutants: the beginning of the molecular genetic analysis of multivesicular body biogenesis. Mol Biol Cell 21, 4057–4060.

Darsow T, Rieder SE, Emr SD (1997). A multispecificity syntaxin homologue, Vam3p, essential for autophagic and biosynthetic protein transport to the vacuole. J Cell Biol 138, 517–529.

De Maziere AM, Muehlethaler K, van Donselaar E, Salvi S, Davoust J, Cerottini JC, Levy F, Slot JW, Rimoldi D (2002). The melanocytic protein Melan-A/MART-1 has a subcellular localization distinct from typical melanosomal proteins. Traffic 3, 678–693.

Duncan LM, Piper S, Dodd RB, Saville MK, Sanderson CM, Luzio JP, Lehner PJ (2006). Lysine-63-linked ubiquitination is required for endolysosomal degradation of class I molecules. EMBO J 25, 1635–1645.

Dunn R, Klos DA, Adler AS, Hicke L (2004). The C2 domain of the Rsp5 ubiquitin ligase binds membrane phosphoinositides and directs ubiquitination of endosomal cargo. J Cell Biol 165, 135–144.

Dupre S, Urban-Grimal D, Haguenauer-Tsapis R (2004). Ubiquitin and endocytic internalization in yeast and animal cells. Biochim Biophys Acta 1695, 89–111.

Epple UD, Suriapranata I, Eskelinen EL, Thumm M (2001). Aut5/Cvt17p, a putative lipase essential for disintegration of autophagic bodies inside the vacuole. J Bacteriol 183, 5942–5955.

Erpapazoglou Z, Froissard M, Nondier I, Lesuisse E, Haguenauer-Tsapis R, Belgareh-Touze N (2008). Substrate- and ubiquitin-dependent trafficking of the yeast siderophore transporter Sit1. Traffic 9, 1372–1391.

Forsberg H, Hammar M, Andreasson C, Moliner A, Ljungdahl PO (2001). Suppressors of ssy1 and ptr3 null mutations define novel amino acid sensor-independent genes in *Saccharomyces cerevisiae*. Genetics 158, 973–988.

Froissard M, Belgareh-Touzé N, Dias M, Buisson N, Camadro JM, Haguenauer-Tsapis R, Lesuisse E (2007). Trafficking of siderophore transporters in *Saccharomyces cerevisiae* and intracellular fate of ferrioxamine B conjugates. Traffic 8, 1601–1616.

Galan JM, Haguenauer-Tsapis R (1997). Ubiquitin lys63 is involved in ubiquitination of a yeast plasma membrane protein. EMBO J 16, 5847–5854.

Galan JM, Moreau V, Andre B, Volland C, Haguenauer-Tsapis R (1996). Ubiquitination mediated by the Npi1p/Rsp5p ubiquitin-protein ligase is required for endocytosis of the yeast uracil permease. J Biol Chem 271, 10946–10952.

Geetha T, Jiang J, Wooten MW (2005). Lysine 63 polyubiquitination of the nerve growth factor receptor TrkA directs internalization and signaling. Mol Cell 20, 301–312.

Giordano F, Bonetti C, Surace EM, Marigo V, Raposo G (2009). The ocular albinism type 1 (OA1) G-protein-coupled receptor functions with MART-1 at early stages of melanogenesis to control melanosome identity and composition. Hum Mol Genet 18, 4530–4545.

Giordano F, Simoens S, Raposo G (2011). Trafficking of the Ocular albinism type 1 (OA1) G protein-coupled receptor is regulated by ubiquitination and ESCRT function. Proc Natl Acad Sci USA 19 108, 11906–11911.

Glickman M, Ciechanover A (2002). The ubiquitin-proteasome proteolytic pathway: destruction for the sake of construction. Physiol Rev 82, 373–428.

Grenson M, Mousset M, Wiame JM, Bechet J (1966). Multiplicity of the amino acid permeases in *Saccharomyces cerevisiae*. I. Evidence for a specific arginine-transporting system. Biochim Biophys Acta 127, 325–338.

Griffith J, Mari M, De Maziere A, Reggiori F (2008). A cryosectioning procedure for the ultrastructural analysis and the immunogold labelling of yeast *Saccharomyces cerevisiae*. Traffic 9, 1060–1072.

Griffith J, Reggiori F (2009). Ultrastructural analysis of Nanogold-labeled endocytic compartments of yeast *Saccharomyces cerevisiae* using a cryosectioning procedure. J Histochem Cytochem 57, 801–809.

Hein C, Springael JY, Volland C, Haguenauer-Tsapis R, Andre B (1995). NPI1, an essential yeast gene involved in induced degradation of Gap1 and Fur4 permeases, encodes the Rsp5 ubiquitin-protein ligase. Mol Microbiol 18, 77–87.

Hicke L, Schubert HL, Hill CP (2005). Ubiquitin-binding domains. Nat Rev Mol Cell Biol 6, 610–621.

Hoeller D *et al*. (2006). Regulation of ubiquitin-binding proteins by monoubiquitination. Nat Cell Biol 8, 163–169.

Huang F, Kirkpatrick D, Jiang X, Gygi S, Sorkin A (2006). Differential regulation of EGF receptor internalization and degradation by multiubiquitination within the kinase domain. Mol Cell 21, 737–748.

Hurley JH, Lee S, Prag G (2006). Ubiquitin-binding domains. Biochem J 399, 361–372.

Isnard AD, Thomas D, Surdin-Kerjan Y (1996). The study of methionine uptake in *Saccharomyces cerevisiae* reveals a new family of amino acid permeases. J Mol Biol 262, 473–484.

Isono E, Katsiarimpa A, Muller IK, Anzenberger F, Stierhof YD, Geldner N, Chory J, Schwechheimer C (2010). The deubiquitinating enzyme AMSH3 is required for intracellular trafficking and vacuole biogenesis in *Arabidopsis thaliana*. Plant Cell 22, 1826–1837.

Iwaki T, Onishi M, Ikeuchi M, Kita A, Sugiura R, Giga-Hama Y, Fukui Y, Takegawa K (2007). Essential roles of class E Vps proteins for sorting into multivesicular bodies in *Schizosaccharomyces pombe*. Microbiology 153, 2753–2764.

Kamsteeg EJ, Hendriks G, Boone M, Konings IB, Oorschot V, van der Sluijs P, Klumperman J, Deen PM (2006). Short-chain ubiquitination mediates the regulated endocytosis of the aquaporin-2 water channel. Proc Natl Acad Sci USA 103, 18344–18349.

Katzmann DJ, Babst M, Emr SD (2001). Ubiquitin-dependent sorting into the multivesicular body pathway requires the function of a conserved endosomal protein sorting complex. ESCRT-I, Cell 106, 145–155.

Katzmann DJ, Odorizzi G, Emr SD (2002). Receptor downregulation and multivesicular-body sorting. Nat Rev Mol Cell Biol 3, 893–905.

Katzmann DJ, Sarkar S, Chu T, Audhya A, Emr SD (2004). Multivesicular body sorting: ubiquitin ligase Rsp5 is required for the modification and sorting of carboxypeptidase S. Mol Biol Cell 15, 468–480.

Kee Y, Lyon N, Huibregtse JM (2005). The Rsp5 ubiquitin ligase is coupled to and antagonized by the Ubp2 deubiquitinating enzyme. EMBO J 24, 2414–2424.

Kee Y, Munoz W, Lyon N, Huibregtse JM (2006). The deubiquitinating enzyme Ubp2 modulates Rsp5-dependent Lys63-linked polyubiquitin conjugates in *Saccharomyces cerevisiae*. J Biol Chem 281, 36724–36731.

Kim BY, Olzmann JA, Barsh GS, Chin LS, Li L (2007a). Spongiform neurodegeneration-associated E3 ligase Mahogunin ubiquitylates TSG101 and regulates endosomal trafficking. Mol Biol Cell 18, 1129–1142.

Kim HC, Huibregtse JM (2009). Polyubiquitination by HECT E3s and the determinants of chain type specificity. Mol Cell Biol 29, 3307–3318.

Kim HC, Steffen AM, Oldham ML, Chen J, Huibregtse JM (2011). Structure and function of a HECT domain ubiquitin-binding site. EMBO Rep 12, 334–341.

Kim Y, Deng Y, Philpott CC (2007b). GGA2- and ubiquitin-dependent trafficking of Arn1, the ferrichrome transporter of *Saccharomyces cerevisiae*. Mol Biol Cell 18, 1790–1802.

Klapisz E, Sorokina I, Lemeer S, Pijnenburg M, Verkleij AJ, van Bergen en Henegouwen PM (2002). A ubiquitin-interacting motif (UIM) is essential for Eps15 and Eps15R ubiquitination. J Biol Chem 277, 30746–30753.

Komander D, Reyes-Turcu F, Licchesi JD, Odenwaelder P, Wilkinson KD, Barford D (2009). Molecular discrimination of structurally equivalent Lys 63-linked and linear polyubiquitin chains. EMBO Rep 10, 466–473.

Kramer LB, Shim J, Previtera ML, Isack NR, Lee MC, Firestein BL, Rongo C (2010). UEV-1 is an ubiquitin-conjugating enzyme variant that regulates glutamate receptor trafficking in *C. elegans* neurons. PLoS One 5, e14291.

Kulathu Y, Akutsu M, Bremm A, Hofmann K, Komander D (2009). Two-sided ubiquitin binding explains specificity of the TAB2 NZF domain. Nat Struct Mol Biol 16, 1328–1330.

Lam MH, Urban-Grimal D, Bugnicourt A, Greenblatt JF, Haguenauer-Tsapis R, Emili A (2009). Interaction of the deubiquitinating enzyme Ubp2 and the e3 ligase Rsp5 is required for transporter/receptor sorting in the multivesicular body pathway. PLoS One 4, e4259.

Lange A, Hoeller D, Wienk H, Marcillat O, Lancelin JM, Walker O (2010). NMR reveals a different mode of binding of the Stam2 VHS domain to ubiquitin and diubiquitin. Biochemistry 1, 48–62.

Lauwers E, Erpapazoglou Z, Haguenauer-Tsapis R, Andre B (2010). The ubiquitin code of yeast permease trafficking. Trends Cell Biol 20, 196–204.

Lauwers E, Jacob C, Andre B (2009). K63-linked ubiquitin chains as a specific signal for protein sorting into the multivesicular body pathway. J Cell Biol 185, 493–502.

Leon S, Erpapazoglou Z, Haguenauer-Tsapis R (2008). Ear1p and Ssh4p are new adaptors of the ubiquitin ligase Rsp5p for cargo ubiquitylation and sorting at multivesicular bodies. Mol Biol Cell 19, 2379–2388.

Levy F, Muehlethaler K, Salvi S, Peitrequin AL, Lindholm CK, Cerottini JC, Rimoldi D (2005). Ubiquitylation of a melanosomal protein by HECT-E3 ligases serves as sorting signal for lysosomal degradation. Mol Biol Cell 16, 1777–1787.

Li JG, Haines DS, Liu-Chen LY (2008). Agonist-promoted Lys63-linked polyubiquitination of the human kappa-opioid receptor is involved in receptor down-regulation. Mol Pharmacol 73, 1319–1330.

Liu XF, Supek F, Nelson N, Culotta VC (1997). Negative control of heavy metal uptake by the *Saccharomyces cerevisiae* BSD2 gene. J Biol Chem 272, 11763–11769.

Luhtala N, Odorizzi G (2004). Bro1 coordinates deubiquitination in the multivesicular body pathway by recruiting Doa4 to endosomes. J Cell Biol 166, 717–729.

Ma YM, Boucrot E, Villen J, Affar el B, Gygi SP, Gottlinger HG, Kirchhausen T (2007). Targeting of AMSH to endosomes is required for epidermal growth factor receptor degradation. J Biol Chem 282, 9805–9812.

Marchese A, Raiborg C, Santini F, Keen JH, Stenmark H, Benovic JL (2003). The E3 ubiquitin ligase AIP4 mediates ubiquitination and sorting of the G protein-coupled receptor CXCR4. Dev Cell 5, 709–722.

Markgraf DF, Ahnert F, Arlt H, Mari M, Peplowska K, Epp N, Griffith J, Reggiori F, Ungermann C (2009). The CORVET subunit Vps8 cooperates with the Rab5 homolog Vps21 to induce clustering of late endosomal compartments. Mol Biol Cell 20, 5276–5289.

Martin-Serrano J (2007). The role of ubiquitin in retroviral egress. Traffic 8, 1297–1303.

Maspero E, Mari S, Valentini E, Musacchio A, Fish A, Pasqualato S, Polo S (2011). Structure of the HECT:ubiquitin complex and its role in ubiquitin chain elongation. EMBO Rep 12, 342–349.

McCullough J, Clague MJ, Urbe S (2004). AMSH is an endosome-associated ubiquitin isopeptidase. J Cell Biol 166, 487–492.

Morvan J, Froissard M, Haguenauer-Tsapis R, Urban-Grimal D (2004). The ubiquitin ligase Rsp5p is required for modification and sorting of membrane proteins into multivesicular bodies. Traffic 5, 383–392.

Newton K *et al*. (2008). Ubiquitin chain editing revealed by polyubiquitin linkage-specific antibodies. Cell 134, 668–678.

Nickerson DP, Brett CL, Merz AJ (2009). Vps-C complexes: gatekeepers of endolysosomal traffic. Curr Opin Cell Biol 21, 543–551.

Nikko E, Andre B (2007). Split-ubiquitin two-hybrid assay to analyze protein-protein interactions at the endosome: application to *Saccharomyces cerevisiae* Bro1 interacting with ESCRT complexes, the Doa4 ubiquitin hydrolase, and the Rsp5 ubiquitin ligase. Eukaryot Cell 6, 1266–1277.

Nikko E, Pelham HR (2009). Arrestin-mediated endocytosis of yeast plasma membrane transporters. Traffic 10, 1856–1867.

Odorizzi G, Babst M, Emr SD (1998). Fab1p PtdIns(3)P 5-kinase function essential for protein sorting in the multivesicular body. Cell 95, 847–858.

Oldham CE, Mohney RP, Miller SL, Hanes RN, O'Bryan JP (2002). The ubiquitin-interacting motifs target the endocytic adaptor protein epsin for ubiquitination. Curr Biol 12, 1112–1116.

Paiva S, Vieira N, Nondier I, Haguenauer-Tsapis R, Casal M, Urban-Grimal D (2009). Glucose-induced ubiquitylation and endocytosis of the yeast Jen1 transporter: role of lysine 63-linked ubiquitin chains. J Biol Chem 284, 19228–19236.

Pinato S, Scandiuzzi C, Arnaudo N, Citterio E, Gaudino G, Penengo L (2009). RNF168, a new RING finger, MIU-containing protein that modifies chromatin by ubiquitination of histones H2A and H2AX. BMC Mol Biol 10, 55.

Polo S, Sigismund S, Faretta M, Guidi M, Capua MR, Bossi G, Chen H, De Camilli P, Di Fiore PP (2002). A single motif responsible for ubiquitin recognition and monoubiquitination in endocytic proteins. Nature 416, 451–455.

Prescianotto-Baschong C, Riezman H (2002). Ordering of compartments in the yeast endocytic pathway. Traffic 3, 37–49.

Raiborg C, Stenmark H (2009). The ESCRT machinery in endosomal sorting of ubiquitylated membrane proteins. Nature 458, 445–452.

Raymond CK, Howald-Stevenson I, Vater CA, Stevens TH (1992). Morphological classification of the yeast vacuolar protein sorting mutants: evidence for a prevacuolar compartment in class E vps mutants. Mol Biol Cell 3, 1389–1402.

Reggiori F, Pelham HR (2001). Sorting of proteins into multivesicular bodies: ubiquitin-dependent and -independent targeting. EMBO J 20, 5176–5186.

Ren J, Kee Y, Huibregtse JM, Piper RC (2007). Hse1, a component of the yeast Hrs-STAM ubiquitin-sorting complex, associates with ubiquitin peptidases and a ligase to control sorting efficiency into multivesicular bodies. Mol Biol Cell 18, 324–335.

Ren X, Hurley JH (2010). VHS domains of ESCRT-0 cooperate in high-avidity binding to polyubiquitinated cargo. EMBO J 29, 1045–1054.

Ruotolo R, Marchini G, Ottonello S (2008). Membrane transporters and protein traffic networks differentially affecting metal tolerance: a genomic phenotyping study in yeast. Genome Biol 9, R67.

Shih SC, Prag G, Francis SA, Sutanto MA, Hurley JH, Hicke L (2003). A ubiquitin-binding motif required for intramolecular monoubiquitylation, the CUE domain. Embo J 22, 1273–1281.

Sierra MI, Wright MH, Nash PD (2010). AMSH interacts with ESCRT-0 to regulate the stability and trafficking of CXCR4. J Biol Chem 285, 13990–14004.

Sikorski RS, Hieter P (1989). A system of shuttle vectors and yeast host strains designed for efficient manipulation of DNA in *Saccharomyces cerevisiae*. Genetics 122, 19–27.

Slot JW, Geuze HJ (2007). Cryosectioning and immunolabeling. Nat Protoc 2, 2480–2491.

Sorrentino V, Scheer L, Santos A, Reits E, Bleijlevens B, Zelcer N (2011). Distinct functional domains contribute to degradation of the low density lipoprotein receptor (LDLR) by the E3 ubiquitin ligase inducible degrader of the LDLR (IDOL). J Biol Chem 286, 30190–30199.

Spence J, Sadis S, Haas AL, Finley D (1995). A ubiquitin mutant with specific defects in DNA repair and multiubiquitination. Mol Cell Biol 15, 1265–1273.

Springael JY, Galan JM, Haguenauer-Tsapis R, Andre B (1999). NH4+-induced down-regulation of the *Saccharomyces cerevisiae* Gap1p permease involves its ubiquitination with lysine-63-linked chains. J Cell Sci 112, 1375–1383.

Starita LM, Lo RS, Eng JK, von Haller PD, Fields S (2012). Sites of ubiquitin attachment in *Saccharomyces cerevisiae*. Proteomics 12, 236–240.

Stawiecka-Mirota M, Pokrzywa W, Morvan J, Zoladek T, Haguenauer-Tsapis R, Urban-Grimal D, Morsomme P (2007). Targeting of Sna3p to the endosomal pathway depends on its interaction with Rsp5p and multivesicular body sorting on its ubiquitylation. Traffic 8, 1280–1296.

Stimpson HE, Lewis MJ, Pelham HR (2006). Transferrin receptor-like proteins control the degradation of a yeast metal transporter. EMBO J 25, 662–672.

Strack B, Calistri A, Gottlinger HG (2002). Late assembly domain function can exhibit context dependence and involves ubiquitin residues implicated in endocytosis. J Virol 76, 5472–5479.

Stringer DK, Piper RC (2011). A single ubiquitin is sufficient for cargo protein entry into MVBs in the absence of ESCRT ubiquitination. J Cell Biol 192, 229–242.

Tanaka N, Kaneko K, Asao H, Kasai H, Endo Y, Fujita T, Takeshita T, Sugamura K (1999). Possible involvement of a novel STAM-associated molecule "AMSH" in intracellular signal transduction mediated by cytokines. J Biol Chem 274, 19129–19135.

Tsirigotis M, Thurig S, Dube M, Vanderhyden BC, Zhang M, Gray DA (2001). Analysis of ubiquitination in vivo using a transgenic mouse model. Biotechniques 31, 120–126, 128, 130.

Urbanowski JL, Piper RC (2001). Ubiquitin sorts proteins into the intralumenal degradative compartment of the late-endosome/vacuole. Traffic 2, 622–630.

Varadan R, Assfalg M, Haririnia A, Raasi S, Pickart C, Fushman D (2004). Solution conformation of Lys63-linked di-ubiquitin chain provides clues to functional diversity of polyubiquitin signaling. J Biol Chem 279, 7055–7063.

Vina-Vilaseca A, Sorkin A (2010). Lysine 63-linked polyubiquitination of the dopamine transporter requires WW3 and WW4 domains of Nedd4–2 and UBE2D ubiquitin-conjugating enzymes. J Biol Chem 285, 7645–7656.

Vitaliano-Prunier A, Menant A, Hobeika M, Geli V, Gwizdek C, Dargemont C (2008). Ubiquitylation of the COMPASS component Swd2 links H2B ubiquitylation to H3K4 trimethylation. Nat Cell Biol 10, 1365–1371.

Volland C, Urban-Grimal D, Geraud G, Haguenauer-Tsapis R (1994). Endocytosis and degradation of the yeast uracil permease under adverse conditions. J Biol Chem 269, 9833–9841.

Weiss ER, Popova E, Yamanaka H, Kim HC, Huibregtse JM, Gottlinger H (2010). Rescue of HIV-1 release by targeting widely divergent NEDD4-type ubiquitin ligases and isolated catalytic HECT domains to Gag. PLoS Pathog 6, e1001107.

Weissman AM (2001). Themes and variations on ubiquitylation. Nat Rev Mol Cell Biol 2, 169–178.

Wiederkehr A, Avaro S, Prescianotto-Baschong C, Haguenauer-Tsapis R, Riezman H (2000). The F-box protein Rcy1p is involved in endocytic membrane traffic and recycling out of an early endosome in *Saccharomyces cerevisiae*. J Cell Biol 149, 397–410.

Woelk T, Oldrini B, Maspero E, Confalonieri S, Cavallaro E, Di Fiore PP, Polo S (2006). Molecular mechanisms of coupled monoubiquitination. Nat Cell Biol 8, 1246–1254.

Xu P, Duong DM, Seyfried NT, Cheng D, Xie Y, Robert J, Rush J, Hochstrasser M, Finley D, Peng J (2009). Quantitative proteomics reveals the function of unconventional ubiquitin chains in proteasomal degradation. Cell 137, 133–145.

Yogosawa S, Hatakeyama S, Nakayama KI, Miyoshi H, Kohsaka S, Akazawa C (2005). Ubiquitylation and degradation of serum-inducible kinase by hVPS18, a RING-H2 type ubiquitin ligase. J Biol Chem 280, 41619–41627.

Yogosawa S, Kawasaki M, Wakatsuki S, Kominami E, Shiba Y, Nakayama K, Kohsaka S, Akazawa C (2006). Monoubiquitylation of GGA3 by hVPS18 regulates its ubiquitin-binding ability. Biochem Biophys Res Commun 350, 82–90.

Ziv I *et al*. (2011). A perturbed ubiquitin landscape distinguishes between ubiquitin in trafficking and in proteolysis. Mol Cell Proteomics 22, doi: 10.1074/mcp.M111.009753.